MSC-07230
Supplement 2

SERVICE PROPULSION SYSTEM
FINAL FLIGHT EVALUATION

National Aeronautics and Space Administration

LYNDON B. JOHNSON SPACE CENTER

Houston, Texas

June 1974

MSC-07230
Supplement 2

APOLLO 16 MISSION REPORT

SUPPLEMENT 2

SERVICE PROPULSION SYSTEM FINAL FLIGHT EVALUATION

PREPARED BY

TRW Systems

APPROVED BY

Glynn S. Lunney
Manager, Apollo Spacecraft Program

NATIONAL AERONAUTICS AND SPACE ADMINISTRATION
LYNDON B. JOHNSON SPACE CENTER
HOUSTON, TEXAS
June 1974

PROJECT TECHNICAL REPORT

APOLLO 16
CSM 113

SERVICE PROPULSION SYSTEM
FINAL FLIGHT EVALUATION

NAS 9-12330 JANUARY 1973

Prepared for
NATIONAL AERONAUTICS AND SPACE ADMINISTRATION
MANNED SPACECRAFT CENTER
HOUSTON, TEXAS

Prepared by
R. J. Smith
S. C. Wood
Applied Mechanics Section
Systems Evaluation Department

NASA/MSC TRW SYSTEMS

Concurred by: Z. D. Kirkland, Head, Systems Analysis Section
Approved by: R.K.M. Seto, Manager, Task E-99

Concurred by: J. Wood, Manager, Service Propulsion Subsystem
Approved by: J. M. Richardson, Head, Applied Mechanics Section

Concurred by: C. W. Yodzis, Chief, Primary Propulsion Branch
Approved by: R. K. Petersburg, Manager, Systems Evaluation Department

TRW SYSTEMS

TABLE OF CONTENTS

LIST OF TABLES

TABLE OF CONTENTS (Continued)

ILLUSTRATIONS

1.0 PURPOSE AND SCOPE

The purpose of this report is to present the results of the postflight analysis of the Service Propulsion System (SPS) performance during the Apollo 16 Mission. This report is a supplement to the Apollo 16 Mission Report. The primary objective of the analysis was to determine the steady-state performance of the SPS under the environmental conditions of actual space flight.

This report covers the additional analyses performed following the compilation of Reference 1. The following items are the major additions and changes to the results reported in Reference 1:

1) The steady-state performance as determined from analysis of the second and sixth burns is presented.
2) The analysis techniques, problems and assumptions are discussed.
3) The flight analysis results are compared to the preflight predicted performance.
4) The propellant utilization and gaging system (PUGS) operation is evaluated in greater detail.
5) The pressurization system performance is discussed.
6) The transient data and performance are included.
7) The estimated propellant consumption is revised.

2.0 SUMMARY

CSM 113 SPS performance for the Apollo 16 Mission was evaluated and found to be satisfactory. The SPS mission duty cycle consisted of six firings for a total duration of 575.3 seconds.

SPS steady-state performance was determined primarily from the analyses of the second (LOI-1) and sixth (TEI) burns. It was determined from these analyses that the engine fuel resistance was approximately 3 percent less than its estimated value based on acceptance test data and post-test reorificing. This compares reasonably well with the mean fuel resistance bias of -5.7 percent determined from postflight analysis of Apollo 9, 10, 11, 12 and 14. Average standard inlet condition engine performance values for the two burns analyzed are as follows: thrust, 20751 pounds; specific impulse, 315.5 seconds; and propellant mixture ratio, 1.599. These values are 0.7 percent greater, 0.2 percent greater, and 0.5 percent less, respectively, than corresponding values computed from the preflight engine model, and are within the $\pm 3\sigma$ uncertainties associated with the preflight values.

The PUGS Mode switch was in the auxiliary position for the transearth insertion burn, allowing data from both the primary and auxiliary gaging systems to be received. The auxiliary gaging data agree well with the primary gaging data. The propellant utilization (PU) valve was in the normal position for all burns. The overall propellant mixture ratio for this mission was 1.626. The predicted mixture ratio for the mission was 1.601. The difference between the actual and predicted mixture ratio was .025 units (1.55 percent) and is well within the allowable limits of ±0.0477 units (±3 percent).

3.0 INTRODUCTION

The Apollo 16 Mission was the sixteenth in a series of flights using Apollo flight hardware and included the fifth lunar landing of the Apollo Program. The Apollo 16 Mission utilized CSM 113 which was equipped with SPS Engine S/N 66 (Injector S/N 137). The engine configuration and expected performance characteristics (Reference 2) are contained in Table 2. Since previous flight results of the SPS have consistently shown the existence of a negative mixture ratio shift, SPS Engine S/N 66 was reorificed to increase the mixture ratio for this mission. Figure 19 shows the propellant unbalance for the two major engine firings compared with the predicted unbalance. Although the unbalance at the end of the TEI burn is significantly different than the predicted unbalance, the propellant mixture ratio was well within its 3σ limits.

The SPS performed six burns during the mission, with a total burn duration of 575.3 seconds. The ignition time, burn duration and velocity gain for each of the six SPS burns are contained in Table 1.

Engine bi-propellant valve bank A was used to start all burns. Valve bank B was utilized during the LOI and TEI burns. During these two burns valve bank B was opened approximately five seconds following valve bank A opening.

The first two SPS burns were no-ullage starts, while the remaining burns were preceded by +X Service Module (SM) reaction control system translation maneuvers to ensure SPS propellant settling.

4.0 STEADY-STATE PERFORMANCE ANALYSIS

Analysis Technique

The major analysis effort for this report was concentrated on determining the steady-state performance of the SPS during the second and sixth burns. The remaining four burns were of insufficient duration to warrant a detailed performance analysis. The performance analysis was accomplished with the aid of the Apollo Propulsion Analysis Program (PAP) which utilizes a minimum of variance technique to "best" correlate the available flight and ground test data. The program embodies error models for the various flight and ground test data that are used as inputs, and by statistical and iterative methods arrives at estimations of the system performance history, propellant weights and spacecraft weight which "best" (minimum-variance sense) reconcile the available data.

Analysis Description

The steady-state performance during the second burn was derived from the PAP analysis of a 280-second segment of the burn. The segment analyzed began approximately 74 seconds following ignition (FS-1). The first 74 seconds of the burn were not included, in order to minimize any errors resulting from data filtering spans which include transient data, and because PUGS data near the start of the burn are not stabilized. The time segment analyzed was terminated approximately 21 seconds prior to SPS shutdown (FS-2) to avoid shutdown transients. The burn segment included propellant crossover (storage tank depletion) which occurred about 255 seconds after ignition. The sixth burn steady-state performance was derived from the PAP analysis of a 92-second segment of the burn. The initial 43 seconds of the burn were excluded from the segment to avoid inclusion of data from the

start transient. The segment was terminated approximately 27 seconds prior to engine cutoff in order to exclude shutdown transient data. The steady-state performance analyses of both burns utilized data from the flight measurements listed in Table 3.

The initial estimated spacecraft damp weight (total spacecraft minus SPS propellant) at ignition of the second burn was 62038 lbm. The initial estimated damp weight at ignition of the sixth burn was 24856 lbm. Both values were based on the postflight weight analysis given in Reference 3.

The initial estimates of the SPS propellants onboard at the beginning of the time segment analyzed for the second burn were extrapolated from the loaded propellant weights presented in Section 5. The initial propellant estimates for the time segment analyzed for the sixth burn were extrapolated from the computed propellants remaining at the end of the time segment analyzed for the second burn. All extrapolations of propellant masses used to establish the initial estimates for a given simulation were performed in an iterative manner using derived flow rates and propellant masses from preceding simulations to ensure that the derived propellant mass history was consistent between the two burns analyzed.

The SPS engine thrust chamber throat area was input to the program as a function of time from ignition for each burn. The assumed throat area time history used in the analysis was based on the characterization presented in Reference 4.

The SPS propellant densities used in the analysis were calculated from propellant sample specific gravity data obtained from KSC, flight propellant temperature data, and flight interface pressures. The temperatures used were based on data from feed-system and engine feedline temperature measurements and were input to the program as functions of time. During

steady-state operation, it was assumed that respective tank bulk temperatures and engine interface temperatures were equal for both oxidizer and fuel.

The PAP simulations were performed using the "Tank Pressure Driven" SPS model. Simply stated, this model utilizes input oxidizer and fuel tank pressure values, as functions of time, for the starting points in computing the pressures and flow rates throughout the system. This method of using input tank pressures (rather than measured tank pressures) as initial estimates for the actual flight tank pressures allows the PAP to utilize all of the available measurement data, including the tank pressures, to determine the "best" (minimum-variance sense) match to the data. The PAP does not allow the driving pressures to be used as measurements. Therefore, if the tank pressure measurement data were used to drive the program the resulting "best" match would not include the weighting of the tank pressure data. The PAP was constrained to follow the shape of the input pressures profiles. The residuals in Figures 2, 3, 12 and 13 show that the input pressures have essentially the same profiles as the measured profiles. The shapes of the tank pressure profiles, in turn, strongly influence the computed thrust shape, and therefore, the calculated acceleration shape. The simulations of both burns, using the input tank pressure yielded negligible computed acceleration shape errors.

Analysis Results

The resulting values of the more significant SPS performance parameters, as determined in the analysis, are presented in Tables 4 and 5. Table 4 contains values for the second burn as computed in the PAP simulation. Values are presented for two time slices, which were selected to show performance before and after crossover. Table 5 contains the flight performance values for the sixth burn from the PAP analysis. The values shown are

for a representative time slice. In both tables, the corresponding preflight predicted values for the same time slice are also shown. All performance values, both predicted and from the PAP analysis, are at the same PU valve position and should be directly comparable.

Based on the values computed for the two burns analyzed, and the qualitative comparison of the data from all six burns, it is concluded that the SPS steady-state performance throughout the entire mission was satisfactory.

The PAP analysis determined that the best match to the available data required that the engine fuel hydraulic resistance be adjusted from the value used in the preflight analysis (Reference 2). The derived fuel resistance was 936.0 $lbf\text{-}sec^2/lbm\text{-}ft^5$ for the second burn and 953.0 $lbf\text{-}sec^2/lbm\text{-}ft^5$ for the sixth burn. The fuel resistance determined from the engine acceptance tests was 892.9 $lbf\text{-}sec^2/lbm\text{-}ft^5$. Based on the acceptance test derived value, the fuel resistance after the post acceptance test reorificing (see Section 2) was estimated to be 969.8 $lbf\text{-}sec^2/lbm\text{-}ft^5$. The flight values derived from the analysis were 3.5 percent less and 1.7 less for the second and sixth burns, respectively, than the estimated reorificed acceptance test value. The flight derived values were 2.4 percent greater and 4.2 percent greater for the second and sixth burns, respectively, than the value (914.5 $lbf\text{-}sec^2/lbm\text{-}ft^5$) used in the preflight prediction. The value used for the prediction was obtained by biasing the estimated reorificed acceptance test value based on postflight experience. An adjustment to the engine oxidizer hydraulic resistance was also required. The flight value derived from the PAP analysis was 484.2 $lbf\text{-}sec^2/lbm\text{-}ft^5$, which is 2.0 percent less than the value derived from acceptance testing and used for the preflight prediction.

Significant biases were found to exist in both interfaces, both propellant tanks, and the chamber pressure measurements. The oxidizer interface pressure measurement (SP0931P) data was found to be biased by approximately -4 to -5 psi. The fuel interface pressure measurement (SP0930P) data was biased -2 psi. Negative interface pressure biases under flow conditions have been observed on previous flights. Reference 11 contains a statistical analysis of the interface pressure biases from the Apollo 9 through Apollo 14 Missions. Based on Reference 11, the expected biases were -3.34 psi and -1.54 psi for oxidizer and fuel interface pressure, respectively. The oxidizer tank pressure measurement (SP0003P) data was biased by +14 to +15 psi which substantiates the belief that the loss of reference pressure from this transducer was the cause of the bias (see Section 6.10). The fuel tank pressure measurement (SP0006P) data was biased by -2 to -3 psi. The engine chamber pressure measurement (SP0661P) was biased by -2 to -4 psi.

The analysis verified that the thrust chamber throat area characterization (Reference 2) was relatively accurate, in that no changes were required to achieve a satisfactory data match for either the second or sixth burn. The second burn PAP analysis indicated that the initial estimates for the spacecraft damp weight needed to be increased by 72 lbm. The sixth burn initial estimates were essentially correct.

The final results of the PAP analysis required a reduction in the oxidizer and fuel loads, as computed from the loading data (Table 6), of 126 lbm and 99 lbm, respectively. Compared to previous missions these are much larger reductions in propellant loads. Several factors exist which indicate that the reductions in propellant loads are reasonable. (1) The derived gaging system data, acceleration, and pressures match the corresponding

telemetry data quite well. (2) One PAP run was made with scale factors applied to the oxidizer and fuel storage tank measurements in order to reduce the residual slopes for these two measurements. The results of this run showed no significant difference in propellant loads, but did show a significant difference in Isp bias (increased by 0.37 sec). (3) PAP runs made where the loads were matched resulted in higher pressure biases, poorer gaging system match, and a much larger Isp bias (approximately 2 sec).

The simulation computed consumption (Table 6) for the whole mission agrees reasonably well with consumption from the reported KSC loads and the gaging system readings at shutdown of the sixth burn. Based on the simulation results, the total oxidizer and fuel consumed were 23487 and 14443 pounds, respectively. The corresponding values computed from the reported loads and the gage readings (accounting for sixth burn shutdown consumption) were 23635 pounds and 14492 pounds. Based on the computed consumption the overall mission mixture ratio was 1.626. Following the end of the sixth burn, the computed usable[1] oxidizer and fuel quantities remaining were 1159 pounds and 988 pounds, respectively. Based on the spacecraft mass at the end of the eighth burn, the estimated SPS ΔV capability remaining was approximately 688 ft/sec[2].

Shown in Figures 1 through 18 are the PAP output plots which present the residuals (differences between the filtered flight data and the program-calculated values) and filtered flight data for the segments of the second and sixth burns analyzed. The figures appear in the following order:

---

(1) Based on unusable quantities of 295.2 pounds and 146.2 pounds of oxidizer and fuel, respectively.

(2) Assumes the PU valve to be in the normal position.

vehicle thrust acceleration, oxidizer tank pressure, fuel tank pressure, oxidizer interface pressure, fuel interface pressure, oxidizer sump tank quantity, fuel sump tank quantity, oxidizer and fuel storage tank quantities (second burn only), and chamber pressure for the second and sixth burn, respectively. The values for slopes and intercepts seen in the upper right-hand corner of these graphs represent the slopes and intercepts on the ordinate of a linear fit of the residual data. The closer these numbers are to zero, the better the match.

A strong indication of the validity of the PAP simulation can be obtained by comparing the thrust acceleration calculated in the simulation to that derived from the Apollo Command Module Computer (CMC) ΔV data transmitted via measurement CG0001V. This comparison is easily made in terms of the previously mentioned residual slope and intercept data. Figures 1 and 11 show the thrust acceleration during the portions of the burns analyzed, as derived from the CMC data, and the residual between the data and program calculated values. The residual time histories have essentially zero means and little, if any, discernible trend. This indicates that the simulations, especially in terms of the computed specific impulse, are relatively valid, although other factors must also be considered in evaluating the simulations.

As observed on previous flights, the measured chamber pressure drifted with burn time during both burns, presumably because of thermal effects on the transducer. A model of the chamber pressure drift was derived in Reference 11 from a regression analysis of the Apollo 8 through 14 chamber pressure residual errors. The recommended model, which is a fifth degree polynomial in burn time from ignition, was incorporated in PAP. The negligible slopes on the chamber pressure residuals shown in Figures 10

and 18, for the second and sixth burn, respectively, indicate that the drift model successfully accounted for the chamber pressure drift, thereby allowing inclusion of the chamber pressure measurement data in the analysis. The analysis program results, however, indicated that large negative errors existed in the measured chamber pressure data for both the burns analyzed. The chamber pressure data for the second and sixth burns were biased by -3.8 psi, and -2.6 psi, respectively. However, the raw data show a bias of -2 psi before and after the second burn, and a bias of -1 psi before and after the sixth burn. This indicates that during both burns the chamber pressure data contained a scale type error of -1.8 to -1.6 psi.

Comparison with Preflight Performance Prediction

Prior to the Apollo 16 Mission, the expected performance of the SPS was presented in Reference 2. This performance prediction was for the integrated propellant feed/engine system and, whenever possible, utilized data and characteristics for the specific SPS hardware on this flight.

The steady-state thrust, propellant mixture ratio, propellant flow rates, and specific impulse are given in Tables 4 and 5 for the second and sixth burn, respectively. Since no PU valve movement occurred during either the predicted simulation or the actual flight, the values shown in these tables can be used for a direct comparison between predicted and derived performance.

Previous flight results have consistently shown the inflight mixture ratio to be significantly less than expected based on the engine acceptance test data. As a result, the majority of SPS burn time was performed with the PU valve in the primary increase position. The purpose of the PU valve is to have the capability of adjusting the average propellant mixture ratio to 1.60 to 1 (which would ensure a minimum propellant outage). Such mixture

ratio shifts, as experienced on previous flights, greatly reduce this capability, and if an even larger shift should occur on future flights, this capability would be non-existent. In order to rectify this situation, North American Rockwell directed Aerojet (Reference 10) to calculate new fuel orifice sizes for Apollo SPS engines S/N 058 and 063 through 072 based on the following conditions:

1) Oxidizer interface orifice to remain unchanged.
2) Engine mixture ratio to be 1.60 to 1.
3) Oxidizer inlet pressure of 162 psia (this is a steady-state flow condition and is unchanged from that value at which the engines were acceptance tested).
4) Fuel inlet pressure of 175 psia (this is also a steady-state flow condition and is increased by 6 psia from that value at which the engines were acceptance tested).

Using the above requirements and the engine acceptance data, the resistance was calculated through the following steps:

1) Using the existing oxidizer resistance, the specified inlet pressures, and the acceptance test value of characteristic exhaust velocity, the chamber pressure calculations were iterated to derive values of oxidizer and fuel flow rates at a mixture ratio of 1.60 to 1 for dual bore.
2) Using the fuel flow rate, the required value of the fuel circuit resistance was calculated. The difference between the existing resistance and the calculated resistance then determined the required increase in the fuel interface orifice.

The reorificed fuel engine feedline resistance for engine S/N 066 was obtained from the above procedure.

In order to more closely predict the expected inflight mixture ratio based on past flight experience, the reorificed engine fuel hydraulic resistance determined from the acceptance test data was biased by -5.7 percent, which decreased the mixture ratio expected with the reorificed fuel hydraulic resistances by 2.9 percent at standard inlet conditions. This bias was obtained by statistically analyzing the results of postflight analyses from Apollo Missions 9, 10, 11, 12 and 14.

Tables 4 and 5 show that the flight reconstructed mixture ratio agrees reasonably well with the predicted mixture ratio. The maximum difference of 0.046 which occurred during the sixth burn is within the preflight uncertainty (Reference 2) of $\pm$ 0.049 (3 sigma). Although this is a significant difference, the overall propellant mixture ratio difference for this mission was 0.0248 units (1.55 percent) and is well within the allowable limits of 0.0477 units (3 percent). Similarly, the reconstructed thrust and specific impulse (Tables 3 and 4) were within the prediction uncertainties of $\pm$ 254 pounds (3 sigma) and $\pm$ 1.59 seconds (3 sigma), respectively.

Engine Performance at Standard Inlet Conditions

The expected flight performance of the SPS engine was based on data obtained during the engine and injector acceptance tests, including data based on the reorificing of the fuel engine feedline (Reference 2). In order to provide a common basis for comparing engine performance, the acceptance test performance is adjusted to standard inlet conditions. This allows actual engine performance variations to be separated from performance variations which are induced by feed-system, pressurization system, and propellant temperature variations.

The standard inlet conditions thrust, specific impulse and propellant mixture ratio from the engine model used in the preflight prediction are 20600 pounds, 314.8 seconds and 1.606, respectively. Based on the steady-state analysis of the second burn, the standard inlet conditions thrust, specific impulse and propellant mixture ratio were 20760 pounds, 315.4 seconds and 1.591, respectively. These values are 0.78 percent greater, 0.19 percent greater and 0.93 percent less, respectively, than the corresponding values computed from the engine model used in the preflight prediction.

The sixth burn analysis yielded standard inlet conditions thrust, specific impulse and propellant mixture ratio of 20742 pounds, 315.6 seconds and 1.606 units, respectively. These values are 0.69 percent greater, 0.25 percent greater and 0.0 percent greater, respectively, than the corresponding values computed from the preflight engine model.

The standard inlet conditions performance values for the two burns agree well with each other, with values for the thrust, specific impulse, and propellant mixture ratio being only 18 pounds, 0.2 seconds, and 0.015 units different, respectively. The average standard inlet conditions thrust, specific impulse and propellant mixture ratio for the two burns were 20751 pounds, 315.5 seconds and 1.599, respectively. These values are 0.7 percent greater, 0.2 percent greater, and 0.5 less, respectively, than the corresponding values computed from the preflight engine model.

As previously discussed, the engine fuel resistance used in the preflight prediction was adjusted from its acceptance test value in an attempt to improve the mixture ratio prediction. If the average standard inlet conditions thrust, specific impulse and mixture ratio from the flight are

compared to their corresponding values computed from an engine model based on the unadjusted acceptance test resistances the values are found to be 0.01 percent less, 0.02 percent greater and 4.0 percent greater, respectively, than the values from the unadjusted model.

The standard inlet conditions performance values reported herein were calculated for the following conditions.

STANDARD INLET CONDITIONS

Oxidizer interface pressure, psia	162
Fuel interface pressure, psia	175
Oxidizer interface temperature, °F	70
Fuel interface temperature, °F	70
Oxidizer density, lbm/ft^3	90.15
Fuel density, lbm/ft^3	56.31
Thrust acceleration, lbf/lbm	1.0
Throat area (initial value), in^2	121.68

Of primary concern in the flight analysis of all Block II engines is the verification of the present methods of extrapolating the specific impulse for the actual flight environment from data obtained during ground acceptance tests at sea level conditions. Since the SPS engine is not altitude tested during the acceptance tests, the expected specific impulse is calculated from the data obtained from the injector sea level acceptance tests using conversion factors determined from Arnold Engineering Developing Center (AEDC) simulated altitude qualification testing. As previously discussed, the average standard inlet conditions specific impulse determined from analyses of the second and sixth burns was 315.5 seconds. The predicted specific impulse at standard inlet conditions, as extrapolated from the ground test was 314.8 seconds. The expected tolerance associated with the predicted standard inlet condition value of 314.8 seconds (Reference 2) was $\pm$ 1.599 seconds (3-sigma). The flight value was well within this tolerance. Therefore, it is concluded that the present methods of extrapolating the expected flight specific impulse from the ground test data were satisfactory for this flight.

5.0 PUGS EVALUATION AND PROPELLANT LOADING

Propellant Loading

The oxidizer tanks were loaded to CM display readout of 100.9 percent at a tank pressure of 110 psia and an oxidizer temperature of 67°F. The fuel tanks were loaded at 108 psia and 68°F to a display readout of 100.9 percent. The SPS propellant loads calculated from these data are shown in Table 6. As planned, the oxidizer storage tank primary gage was zero adjusted with a nominal -0.4 percent bias. This zero adjustment bias was incorporated for Apollo 10 and subsequent missions to prevent erroneous storage tank readings after crossover as experienced during the Apollo 9 Mission (Reference 4). The zero adjustment bias causes a small, but known, time varying error (a -0.4 percent bias and a +0.8 percent scale factor) in the readings from the storage tank primary gage prior to crossover.

PUGS Operation in Flight

The propellant utilization gaging system (PUGS) operated satisfactorily throughout the mission. During the descent orbit insertion burn, the gaging system erroneously indicated approximately 1.5 percent propellant remaining in the empty oxidizer storage tank. Subsequent to the DOI burn, telemetry data received from the lunar orbit plane change burn show that the oxidizer storage tank had the correct value of 0.0 percent propellant remaining. The PUGS Mode switch was in the auxiliary position for the transearth insertion burn, thus, allowing data from both the primary and auxiliary gaging systems to be received. The auxiliary gaging data agree well with the primary gaging data. The propellant utilization (PU) valve was in the normal position at launch and remained in normal throughout the flight.

Figure 19 shows the indicated propellant unbalance history for the second and sixth burns; as computed from the filtered T/M PUGS data. The indicated unbalance history should reflect the CM display unbalance history, within the T/M accuracy. The T/M indicated unbalance at the end of the eighth burn was 435 pounds decrease. The expected unbalance which is also shown in Figure 19 is seen to differ significantly with the actual. However, as discussed in Section 4, the mixture ratio was within the 3σ allowable limits. As expected, based on past flights, the indicated unbalance following the start of the second burn showed decrease readings. The initial readings are caused by three factors: 1) the previously mentioned -0.4 percent calibration bias on the oxidizer storage tank probe, 2) ungageable oxidizer (approximately 100 pounds) above the top of the oxidizer sump tank probe prior to crossover due to propellant transfer from helium absorption, and 3) the tendency of the fuel probes to read erroneously high for about 30-40 seconds following ignition of low acceleration burns due to capillary action in the probe stillwells. The first two error sources are accounted for in the preflight model, resulting in the initial 115 pound decrease reading shown (Figure 19) for the expected unbalance. Because the third error source (the erroneously high fuel probe readings near the ignition transient) caused errors of relatively short duration, no attempt was made to account for this phenomenon in the preflight model. After propellant crossover, at about 255 seconds into the second burn, the unbalance is seen to take a step increase as the effects of the two known oxidizer sump tank gaging errors (the -0.4 percent bias and the oxidizer above the sump tank probe) are eliminated.

6.0 PRESSURIZATION SYSTEM EVALUATION

Operation of the helium pressurization system was satisfactory without any indication of leakage. The helium supply pressures indicated nominal helium usage for the six SPS burns.

After liftoff the oxidizer tank pressure (SP0003) and oxidizer engine inlet pressure (SP0931) were indicating normal levels of 175 psia and 174 psia, respectively. Indicated oxidizer pressure then increased by 2 psi in a period of three hours. Oxidizer pressure and both fuel pressures indicated normal levels. After the separation, docking, and LM extraction maneuvers, it is normal to expect a decay in tank pressures due to absorption of the ullage gas into the propellant. The expected decay was noted on the oxidizer interface pressure which decayed from 174 psia to 164 psia at AET 30:28:00. The tank pressure indication, however, remained at 175 psia and indicated a gradual pressure rise to 177 at AET 30:20:00.

At this point it was suspected that the SP0003 pressure transducer was leaking gas from the reference cavity which is pressurized at ambient pressure (14.7 psia). A slow leak in this cavity would cause a gradual increase in indicated pressure. This failure mode has occurred in previous flights. This particular transducer had also not received a leak check prior to flight because it was installed after the altitude test at KCS. It was decided to raise the tank pressure to regulator lock-up level to evaluate this suspected failure mode. If the tank pressure indicated the same delta pressure with respect to SP0931 and if SP0931 indicated the expected lock-up pressure levels, it would indicate that the tank pressure measurement was shifting to the high side. If the shift continued until a delta pressure of 14 to 15 psi was noted but did not increase beyond that point, the failure mode would have to be loss of reference pressure in the cavity.

The tank pressure was raised to the regulator lock-up level by manually cycling the helium isolation valves and allowing the regulators to flow until it was locked up. The resulting tank pressure was 186 psi as indicated by the interface pressure and verified by readings of 184 and 187 on fuel tank and fuel interface pressure. The oxidizer tank pressure measurement, however, indicated 198 psia. This indicated that the transducer had taken a permanent shift and the delta was the same as noted prior to the manual pressurization. During the remainder of the flight the delta pressure remained between 14 and 16 psi.

The GN_2 actuation system pressures indicated satisfactory usage. At launch the storage pressures for GN_2 Systems A and B were 2440 psi and 2500 psi, respectively. Following the sixth and final SPS burn the T/M data indicated that the System A pressure was 2110 psi and that the System B pressure was 2300 psia. System A was utilized on six SPS burns for an indicated average pressure decrease of approximately 66 psi per burn. System B was utilized on two burns for an indicated average pressure decrease of 100 psi per burn.

The helium pressurization system functioned normally throughout the mission. The helium storage bottles were loaded with 86.6 lbm of helium. The SPS burns used 62.6 lbm for propellant tank pressurization and 24 lbm of helium was left in the storage bottles at the end of the TEI burn.

7.0 ENGINE TRANSIENT ANALYSIS

A summary of the start and shutdown transient performance data for all SPS firings, except for the fifth firing for which no data is available, is presented in Table 7. The difference between burns 1 and 2, and the remaining burns exceeded the start impulse run-to-run specification limits of ±200 lbf-sec, but were within the instrumentation accuracies. The start times (ignition to 90 percent of steady-state thrust) for each burn were all within the specification limits. The computed shutdown impulse for burns 3 and 4 were slightly below the specification limit of 11,000 lbf-sec. All burns exceeded run-to-run specification limits of ±500 lbf-sec, except for burns 3 and 4. The shutdown time (cutoff to 10 percent of steady-state thrust) for each burn were all within specification limits.

The chamber pressure overshoot values for burns 1 and 2 exceeded the specification limit of 120 percent; however, there were no indications of rough combustion or other abnormal performance.

8.0 REFERENCES

1. NASA Report MSC 07230, "Apollo 16 Mission Report," August 1972.

2. Spacecraft Operational Data Book, SNA-8-D-027, Vol. I, Part 1, Amendment 92, 27 March 1972.

3. Spacecraft Operational Data Book, SNA-8-D-027, Vol. III, Amendment 125, 14 April 1972.

4. TRW Technical Report 11176-H311-R0-00, "Apollo 9 CSM 104 Service Propulsion System Final Flight Evaluation," 4 August 1969.

5. TRW Technical Report 11176-H526-R0-00, "Apollo 10 CSM 106 Service Propulsion System Final Flight Evaluation," 31 March 1970.

6. TRW Technical Report 17618-H019-R0-00, "Apollo 11 CSM 107 Service Propulsion System Final Flight Evaluation," September 1970.

7. TRW Technical Report 17618-H058-R0-00, "Apollo 12 CSM 108 Service Propulsion System Final Flight Evaluation," November 1970.

8. TRW Technical Report 17618-H214-R0-00, "Apollo 14 CSM 110 Service Propulsion System Final Flight Evaluation," September 1971.

9. TRW Technical Report 17618-H129-R0-00, "Apollo Primary Propulsion System Engineering Mathematical Models," March 1971.

10. Aerojet General CEM 380, "N[illegible] Fuel Interface Orifices for Apollo SPS Engines 058, 063 through 072," received MSC 4 January 1971.

11. TRW IOC 71.4915.2-61, "Service Propulsion System (SPS) Characterization," 25 October 1971.

TABLE 1

APOLLO 16 SPS DUTY CYCLE

MANEUVER	FS1 (A.E.T.)	FS2 (A.E.T.)	BURN DURATION (SEC)	VELOCITY CHANGE (FT/SEC)
MCC-1	30:39:00.67	30:39:02.67	2.00	12.5
LOI	74:28:27.87	74:34:42.77	374.90	2802.0
DOI	78:33:45.04	78:34:09.39	24.35	209.5
CIRC	103:21:43.08	103:21:47.74	4.66	81.6
LOPC	169:05:51.49	169:05:58.59	7.10	124.0
TEI	200:21:33.06	200:24:15.35	162.29	3370.9
			575.30	6600.5

TABLE 2

CSM 113 SPS ENGINE AND FEED SYSTEM CHARACTERISTICS

Engine No.	66
Injector No.	137
Chamber No.	330
Initial Chamber Throat Area (in^2)	121.6803

Engine and System Fluid Resistances ($lbf\text{-}sec^2/lbm\text{-}ft^5$)

	Based on Acceptance Test	Based on Reorificing	Adjusted
Fuel Engine Feedline	892.9	969.8	914.5
Oxidizer Engine Feedline	494.2		
Fuel System Feedline	36.08		
Oxidizer System Feedline			
PU Valve in the Pri-normal Positon	97.72		
PU Valve in Pri-increase	49.79		
PU Valve in Pri-decrease Position	169.29		

Characterization Equation for C*:

$$C^* = C^*_{S.C.} + 870.5\,(MR - 1.6) - 273.83\,(MR^2 - 2.56) - 0.31878\,(P_C - 99)$$
$$+12.953\,(TP - 70) - 0.07414\,(TP^2 - 4900) - 5.466\,(MR \cdot TP - 112)$$
$$+0.03119\,(MR \cdot TP^2 - 7840.);$$

where $C^*_{S.C.}$ (Engine No. 66) = 5956.4 ft/sec

Characterization Equation for Isp:

$$I_{SP} = I_{SP_{vac}} - 96.954\,(1.6 - MR) - 0.0487\,(99 - P_C) - 0.06276\,(70 - TP)$$
$$+ 30.409\,(2.56 - MR^2) + 0.0004483\,(4900 - TP^2);$$

Where $I_{SP_{vac}}$ (Engine No. 66) = 314.8 lbf-sec/lbm

TABLE 3

FLIGHT DATA USED IN STEADY-STATE ANALYSIS

Measurement Number	Description	Range	Sample Rate Samples/Sec
SP0930 P	Pressure, Engine Fuel Interface	0 to 300 psia	10
SP0931 P	Pressure, Engine Oxidizer Interface	0 to 300 psia	10
SP0661 P	Pressure, Engine Chamber	0 to 150 psia	100
SP0003 P	Pressure, Oxidizer Tanks	0 to 250 psia	10
SP0006 P	Pressure, Fuel Tanks	0 to 250 pisa	10
SP0048 T	Temperature, Engine Fuel Feed Line	0 to 200 °F	1
SP0049 T	Temperature, Engine Oxidizer Feed Line	0 to 200 °F	1
SP0056 T	Temperature, 1 Fuel Distribution Line	0 to 200 °F	1
SP0655 Q	Quantity, Oxidizer Tank 1 Primary - Total Auxiliary	0 to 50%	1
SP0656 Q	Quantity, Oxidizer Tank 2	0 to 60%	1
SP0657 Q	Quantity, Fuel Tank 1 Primary - Total Auxiliary	0 to 50%	1
SP0658 Q	Quantity, Fuel Tank 2	0 to 60%	1
CG0001 V	Computer Digital Data	40 Bits	1/2

TABLE 4

APOLLO 16

SERVICE PROPULSION SYSTEM STEADY-STATE PERFORMANCE
SECOND SPS BURN
(LOI)

PARAMETER	INSTRUMENTED					
	Before Crossover			After Crossover		
	FS-1 + 104 sec.			FS-1 + 314 sec.		
	Predicted[1]	PAP[2]	Measured[3]	Predicted[1]	PAP[2]	Measured[3]
PU Valve Position	Normal	Normal	Normal	Normal	Normal	Normal
Oxidizer Tank Pressure, Psia	178	175	190	178	177	191
Fuel Tank Pressure, Psia	178	177	174	178	179	176
Ox Interface Pressure, Psia	164	161	157	166	166	162
Fuel Interface Pressure, Psia	174	173	171	176	177	175
Engine Chamber Pressure, Psia	101	102	98	102	105	101
	DERIVED					
Oxidizer Flow rate, lbm/sec	40.5	40.5	---	41.1	41.3	---
Fuel Flow rate, lbm/sec	25.5	25.1	---	25.6	25.4	---
Propellant Mixture Ratio	1.590	1.615	---	1.601	1.624	---
Vacuum Specific Impulse, Sec	314.9	315.4	---	315.0	315.4	---
Vacuum Thrust, lbf	20796	20688	---	21004	21051	---

Notes:
1. Predicted values from Reference 2.
2. Derived values from Propulsion Analysis Program.
3. Measured data are as recorded and are not corrected for biases and errors discussed in text.

TABLE 5

APOLLO 16

SERVICE PROPULSION SYSTEM STEADY-STATE PERFORMANCE
SIXTH SPS BURN
(TEI)

PARAMETER	INSTRUMENTED FS-1 + 83 Sec.		
	Predicted[1]	PAP[2]	Measured[3]
PU Valve Position	Normal	Normal	Normal
Oxidizer Tank Pressure, Psia	178	177	192
Fuel Tank Pressure, Psia	179	178	176
Oxidizer Interface Pressure, Psia	167	166	161
Fuel Interface Pressure, Psia	177	176	174
Engine Chamber Pressure, Psia	102	103	101
DERIVED			
Oxidizer Flow rate, lbm/sec	41.2	41.4	---
Fuel Flow rate, lbm/sec	25.7	25.1	---
Propellant Mixture Ratio	1.603	1.649	---
Vacuum Specific Impulse, sec	315.0	315.6	---
Vacuum Thrust, lbf	21048	21012	---

Notes:
1. Predicted values from Reference 2.
2. Derived values from Propulsion Analysis Program.
3. Measured data are as recorded and are not corrected for biases and errors discussed in text.

TABLE 6

APOLLO 16

SPS PROPELLANT DATA

Total Mass Loaded (lbm)

Propellant	Computed from Loading Data	Based on Analysis
Oxidizer	25070.	24772
Fuel	15676.	15577.
TOTAL	40746.	40519.

Propellant Consumption (lbm)

Propellant	Computed from Loading Data and PUGS[1]	Analysis Results
Oxidizer	23635.	23487.
Fuel	14492.	14443.
TOTAL	38127.	37930.

Propellant Residuals (lbm)

Propellant	Computed from PUGS[1]	Analysis Results
Usable Oxidizer	1140.	1159.
Usable Fuel	1039.	988.
TOTAL	2179.	2147.

(1) Crew reported CMC panel readings.

TABLE 7

APOLLO 16

ENGINE TRANSIENT DATA

PARAMETER	SPECIFICATION VALUE		APOLLO 16 SPS MANEUVERS				
	Single Bore	Dual Bore	1st	2nd	3rd	4th	6th
Total Vacuum Impulses (Ignition to 90% Steady-State Thrust), lbf-sec	450 ±250 (1) ±200 (2)	568	293	507	584	312	423
Time (Ignition to 90% Steady-State Thrust), sec	0.675 ±0.100		.574	.661	.640	.625	.659
Chamber Pressure Overshoot, Percent	120		124	133	109	114	120
Total Vacuum Impulse (Cutoff to 0% Steady-State Thrust), lbf-sec	12,500 ± 2,500 (1) ± 500 (2)	13,500 2,500 (1) 500 (2)	12,678	13,698	10,550	10,836	14,464
Time (Cutoff to 10% Steady-State Thrust), sec	1.075	1.075	0.756	1.043	0.923	0.901	1.025

(1) Engine-to-Engine Tolerance
(2) Run-to-Run Tolerance

FOLDOUT FRAME

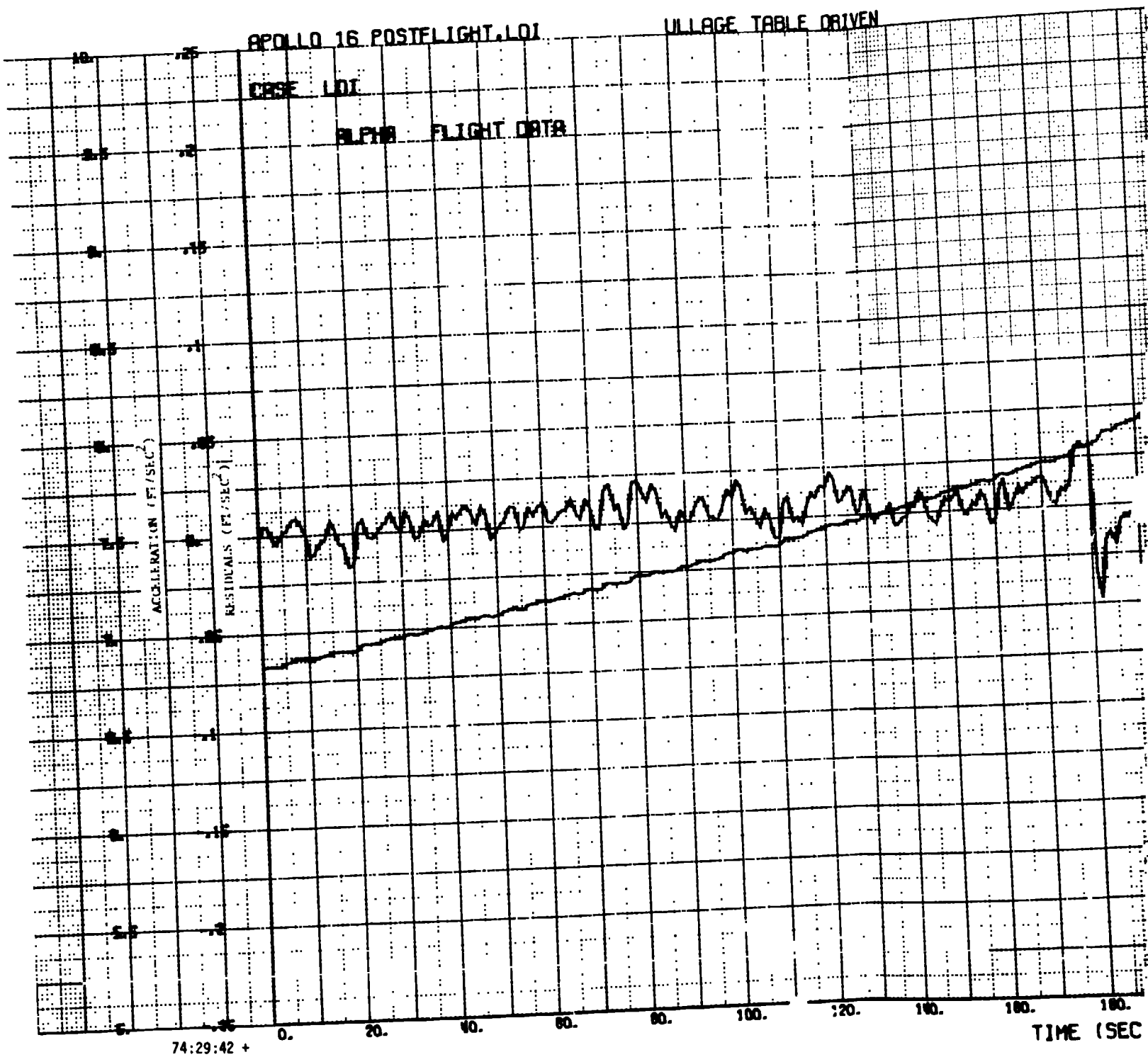

FOLDOUT FRAME 2

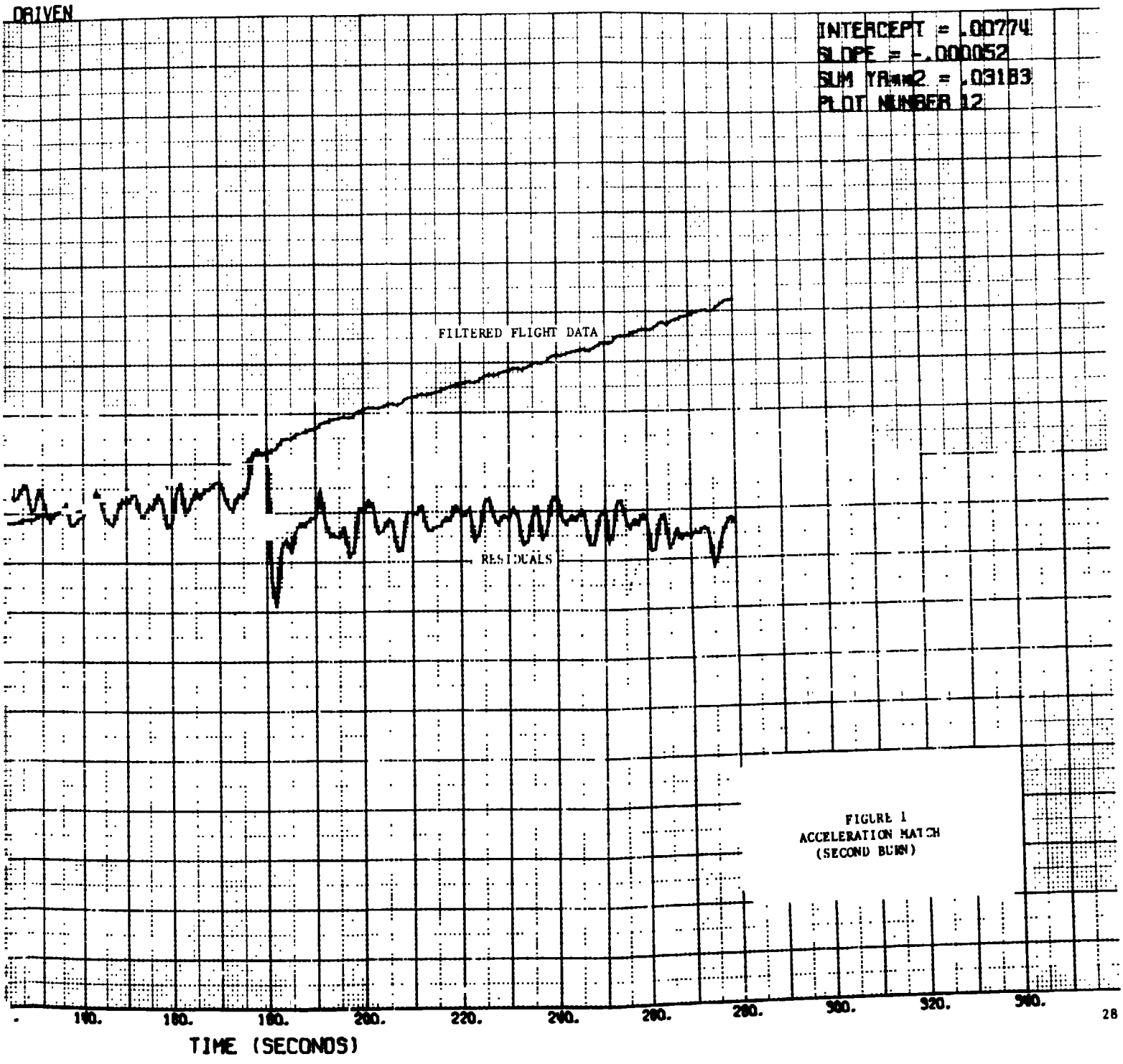

FIGURE 1
ACCELERATION MATCH
(SECOND BURN)

BLOWOUT FRAME

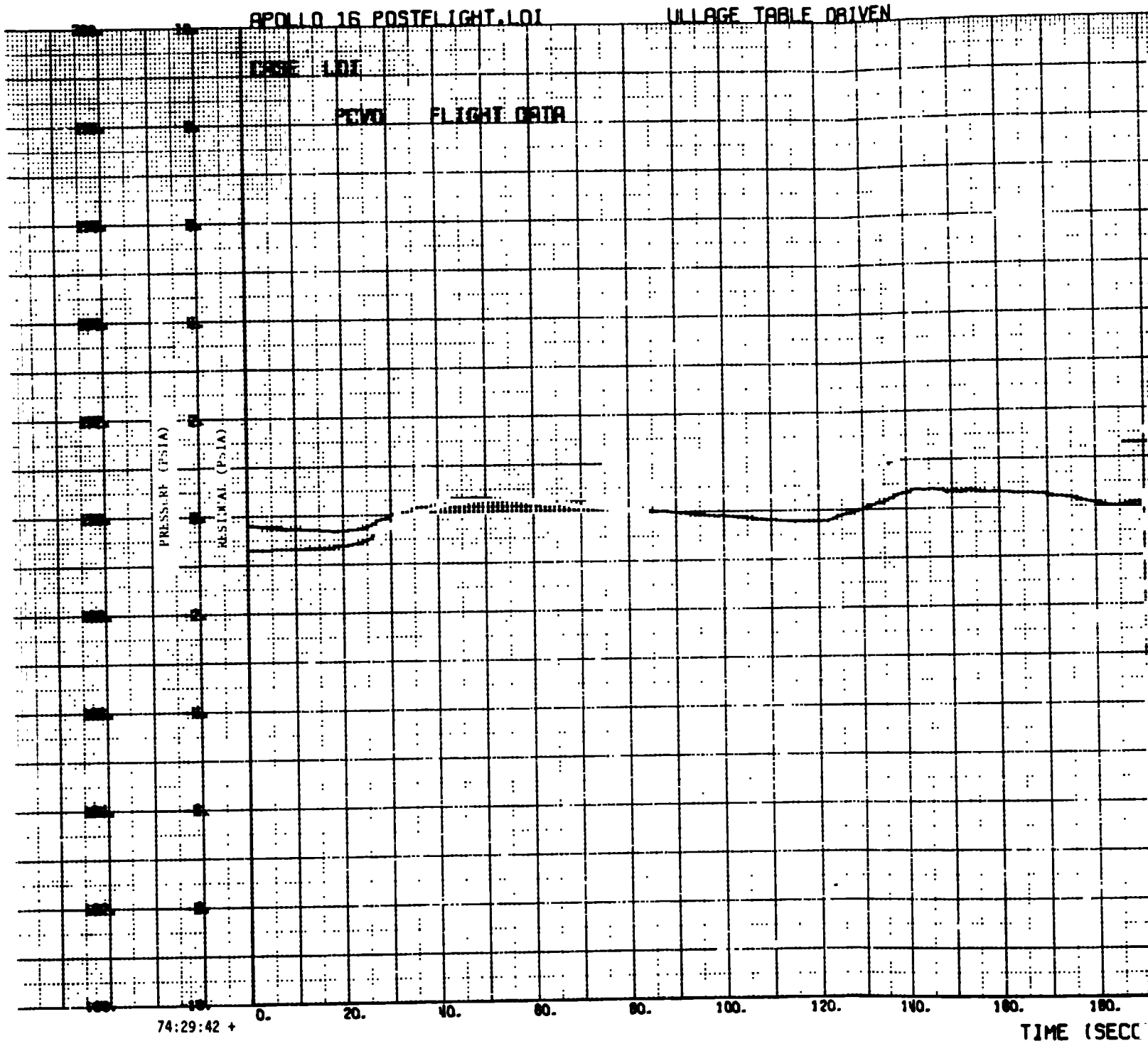

FOLDOUT FRAME

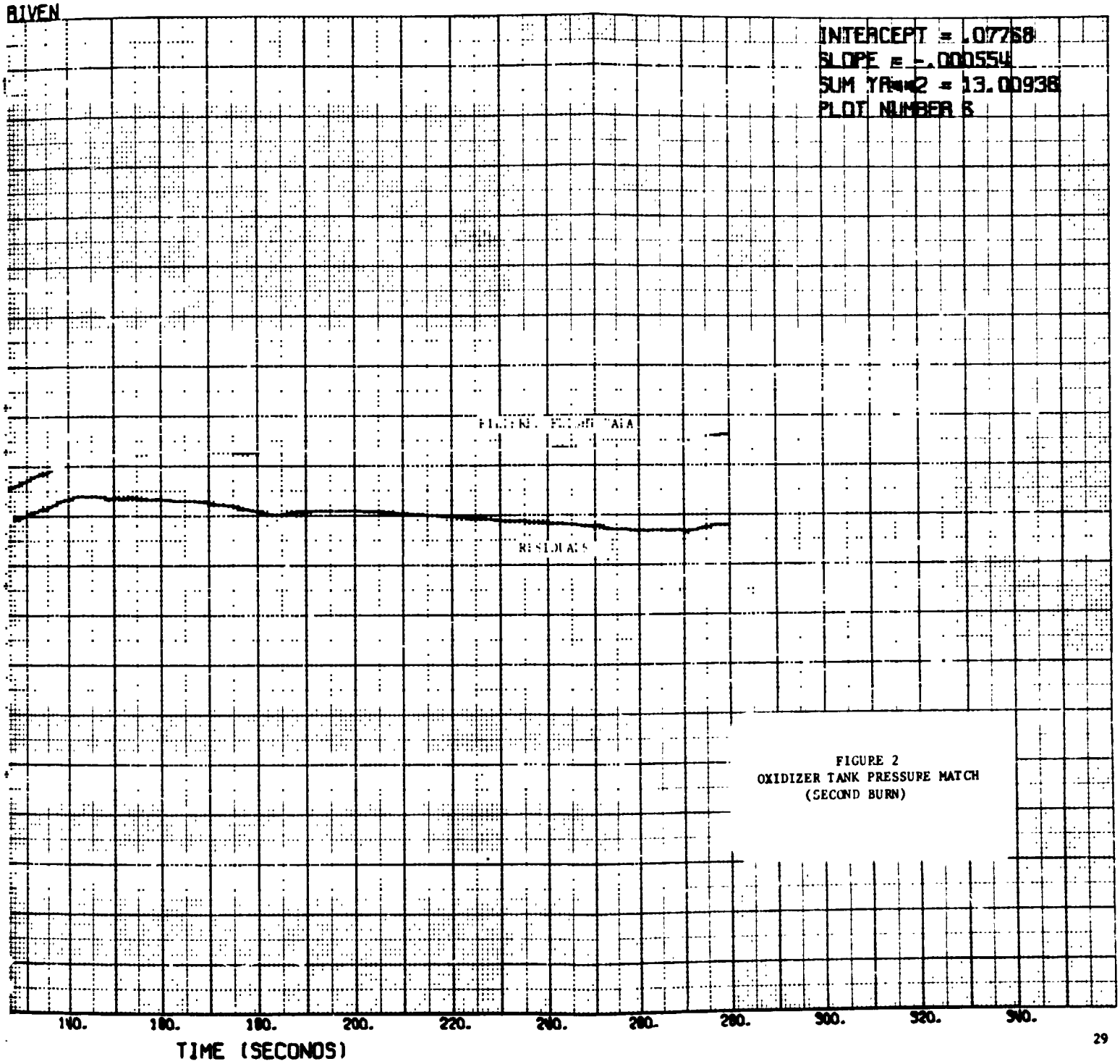

FIGURE 2
OXIDIZER TANK PRESSURE MATCH
(SECOND BURN)

FOLDOUT FRAME

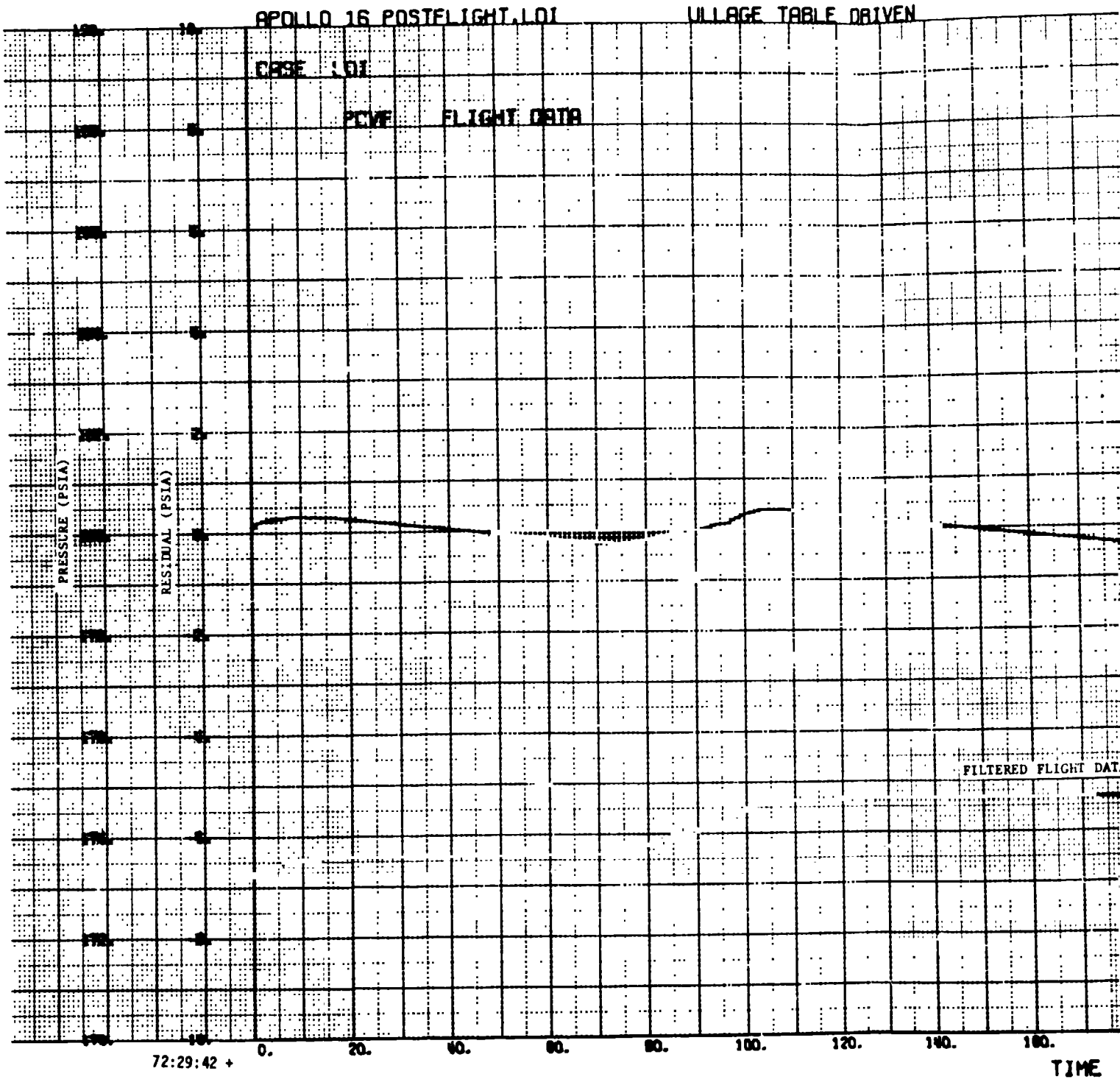

FOLDOUT FRAME 2

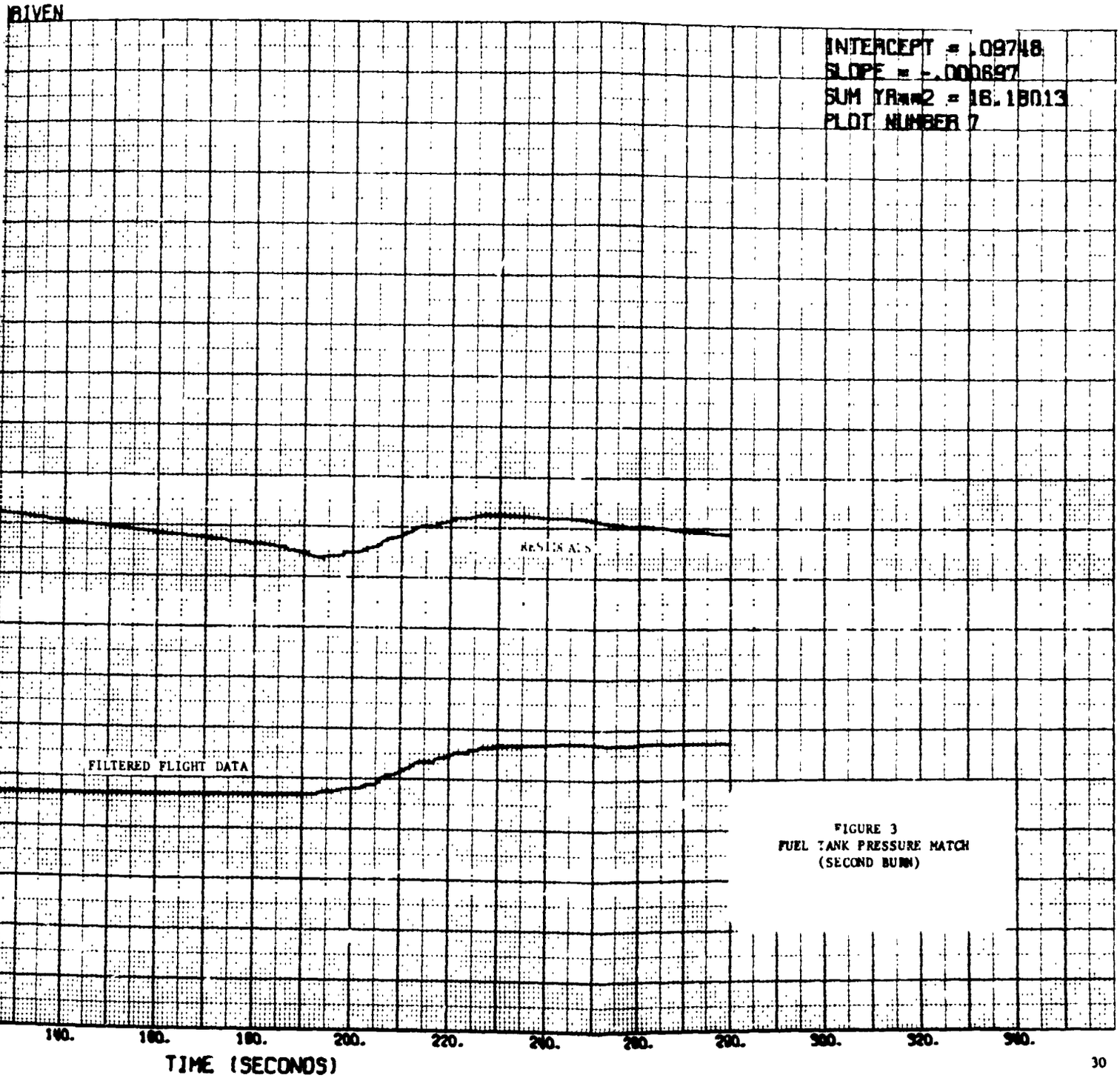

FIGURE 3
FUEL TANK PRESSURE MATCH
(SECOND BURN)

FOLDOUT FRAME

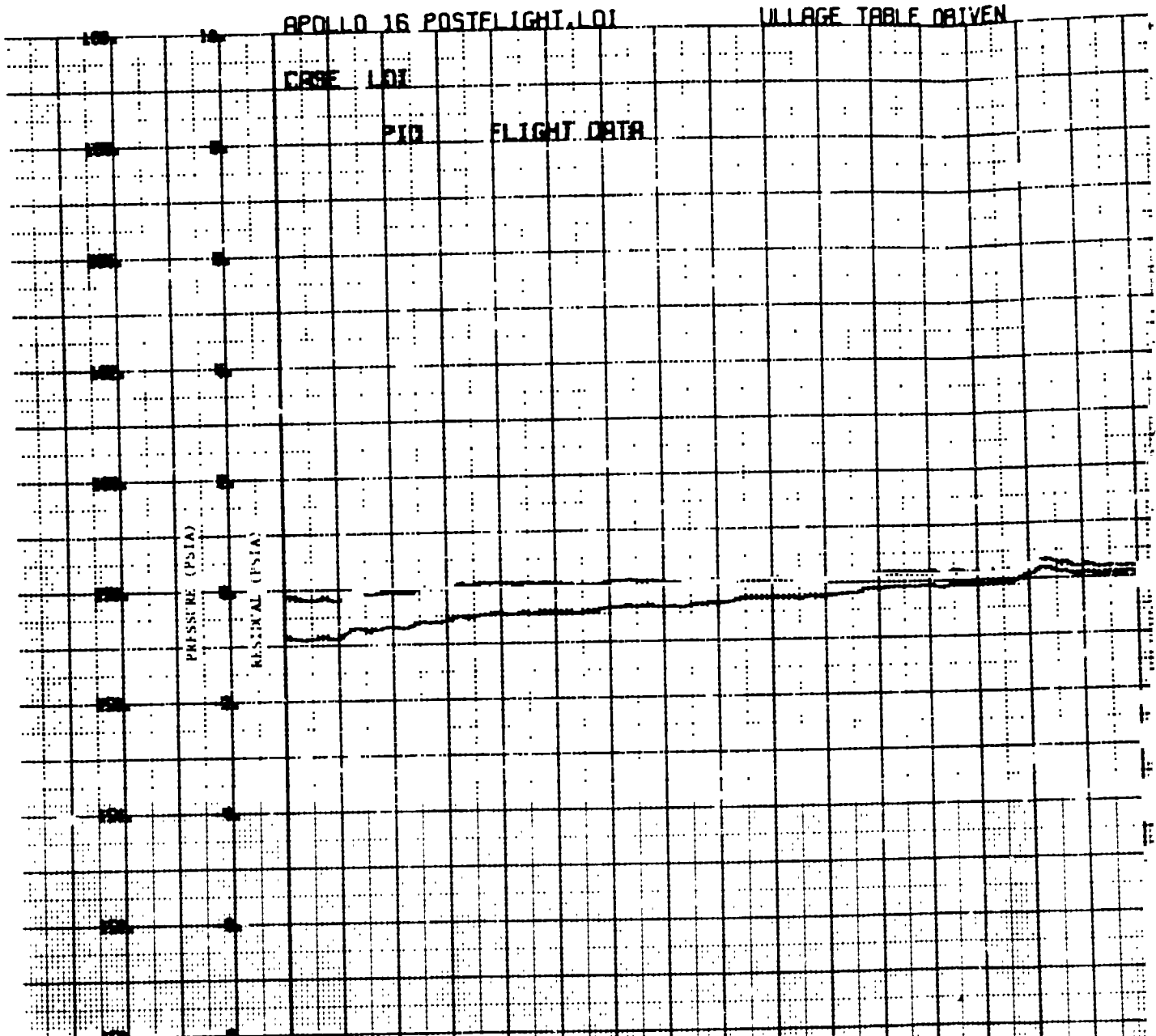

FOLDOUT FRAME 2

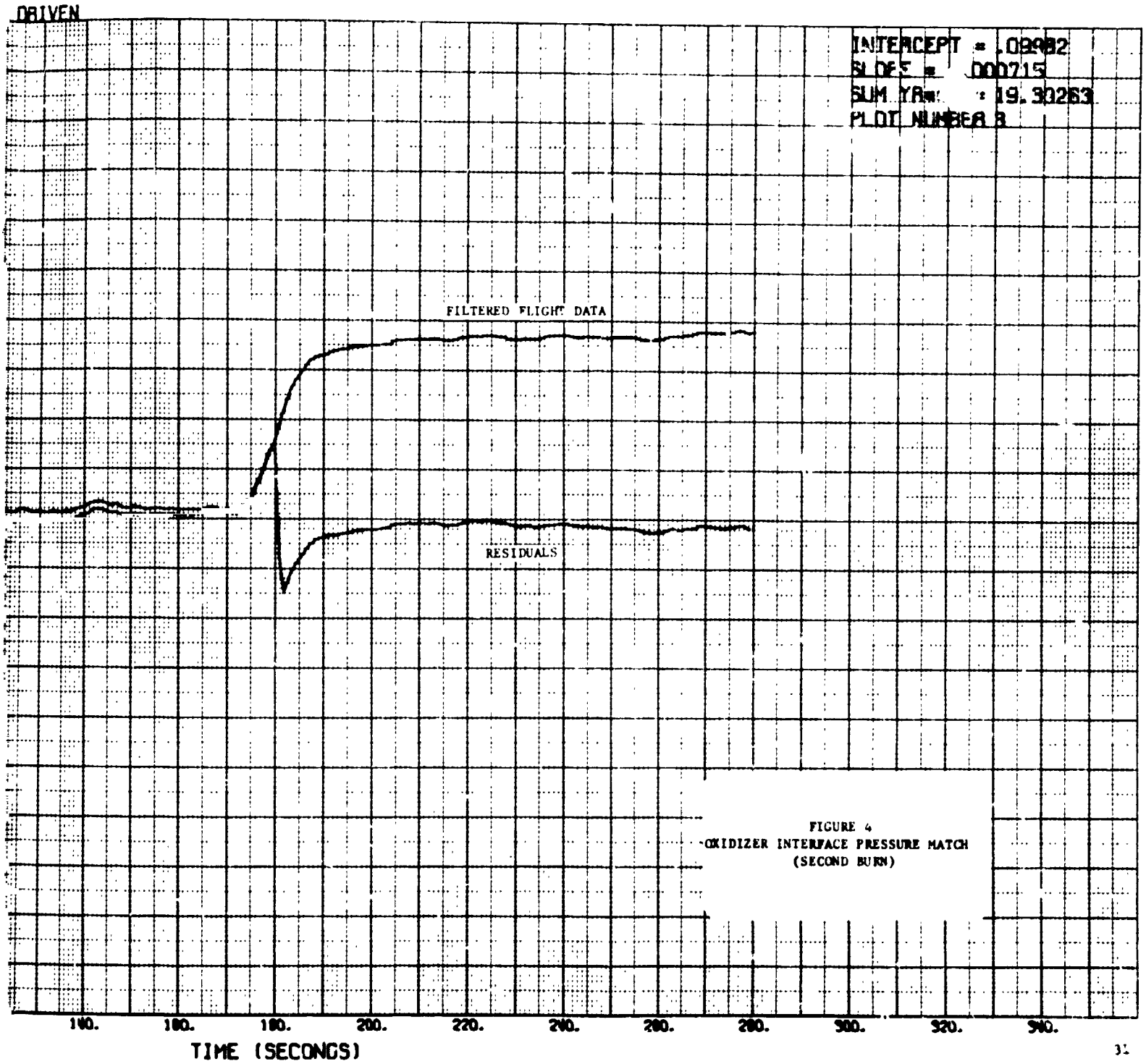

FIGURE 4
OXIDIZER INTERFACE PRESSURE MATCH
(SECOND BURN)

FOLDOUT FRAME

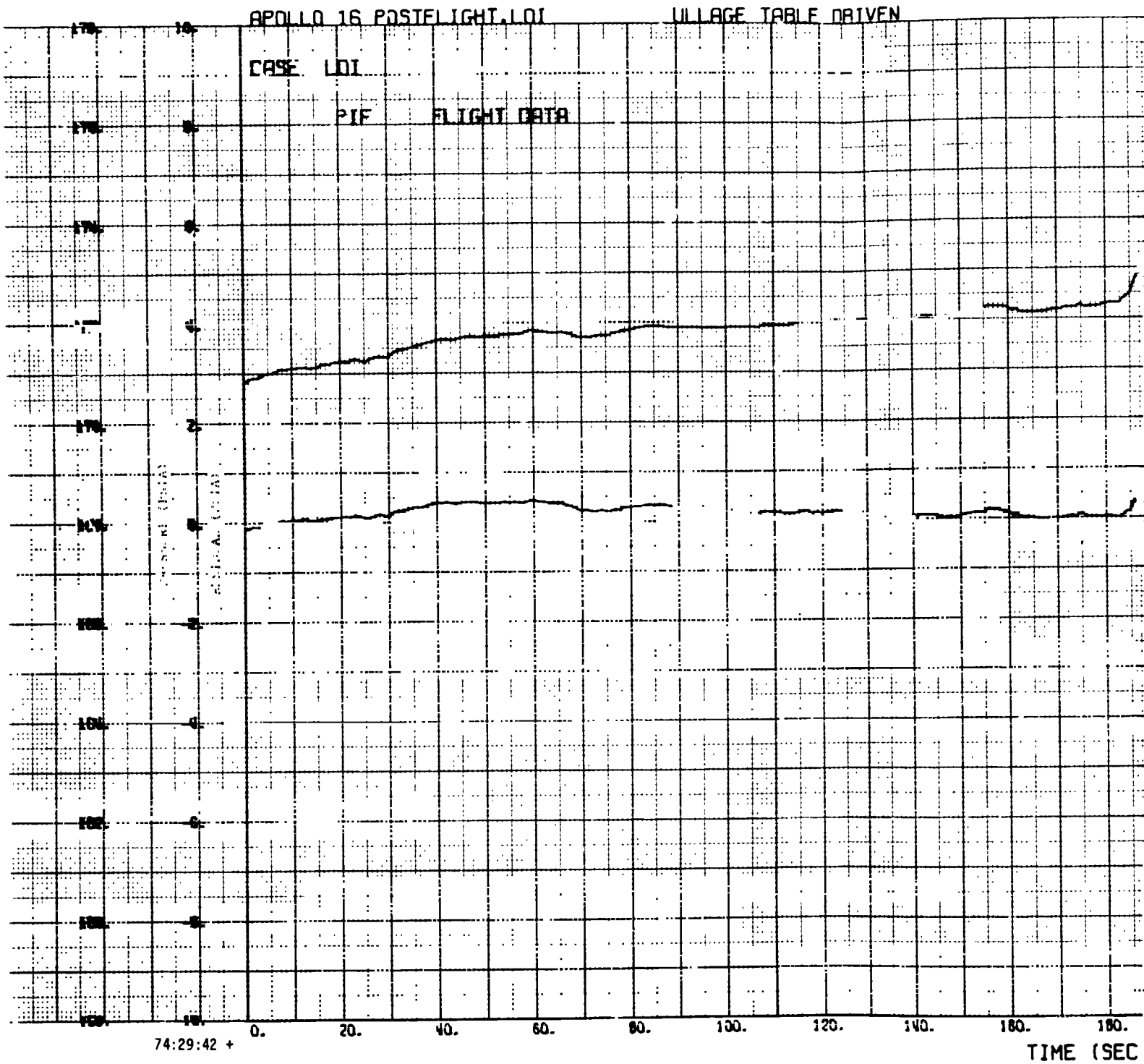

FOLDOUT FRAME 2

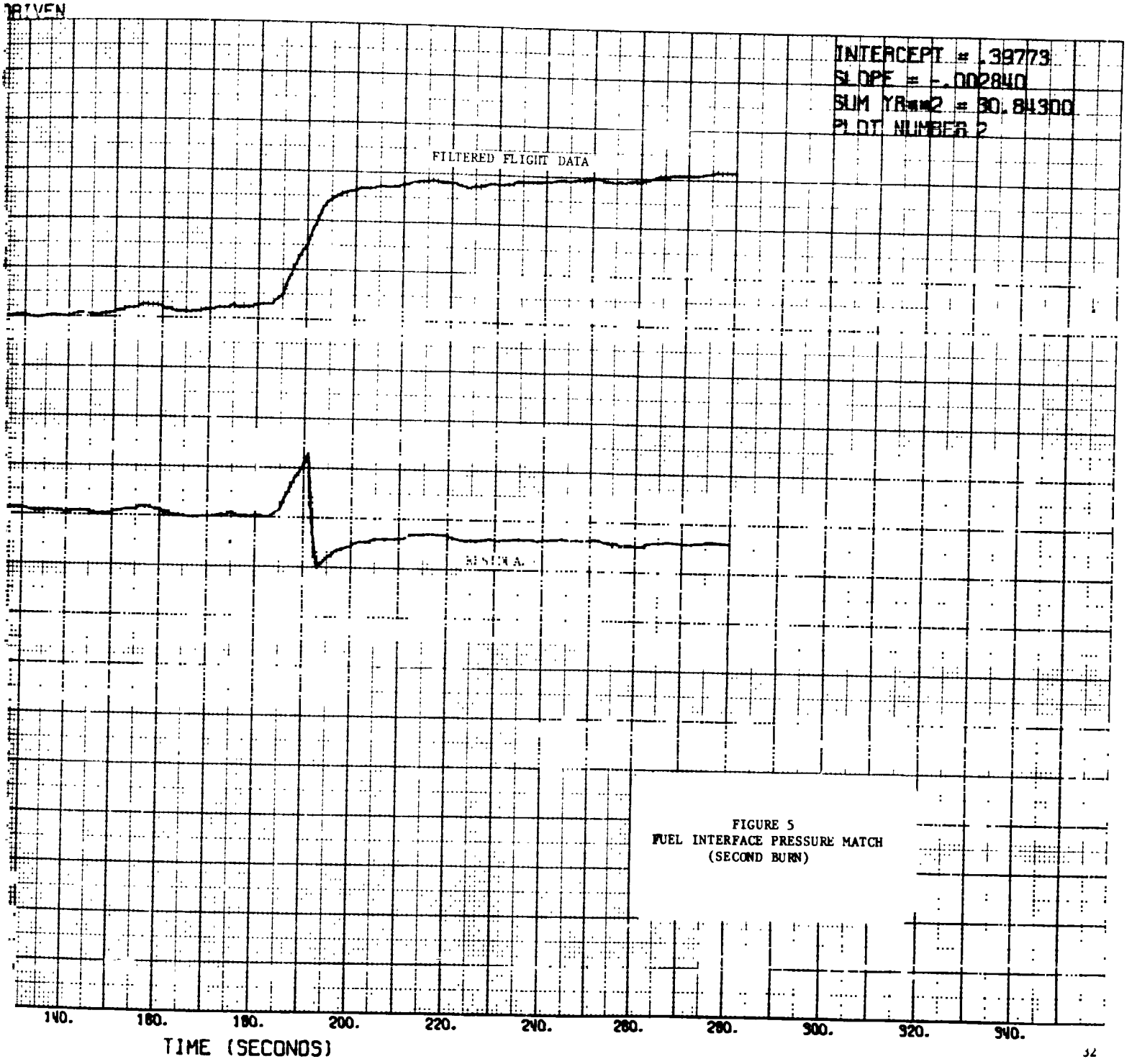

FIGURE 5
FUEL INTERFACE PRESSURE MATCH
(SECOND BURN)

FOLDOUT FRAME

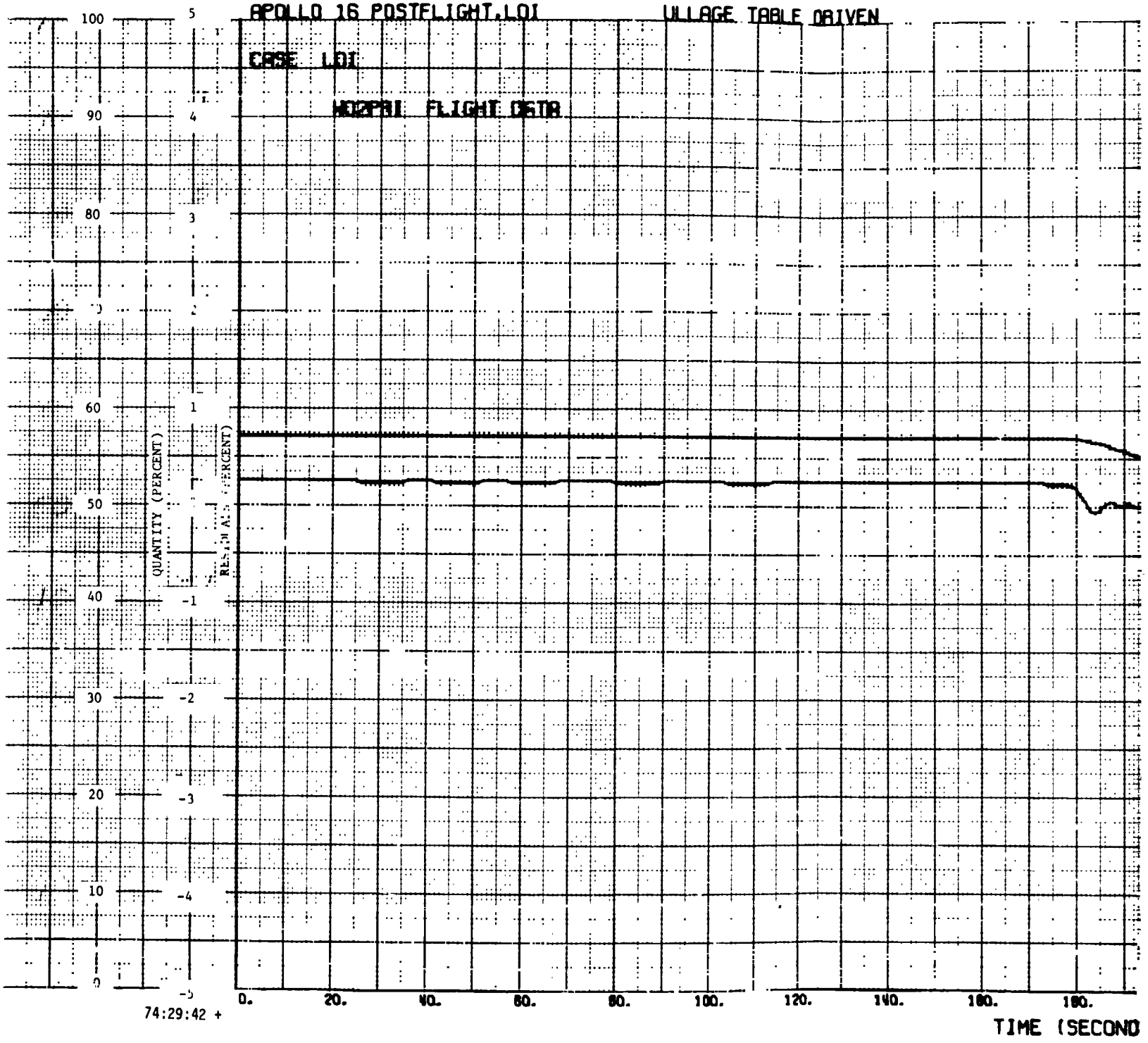

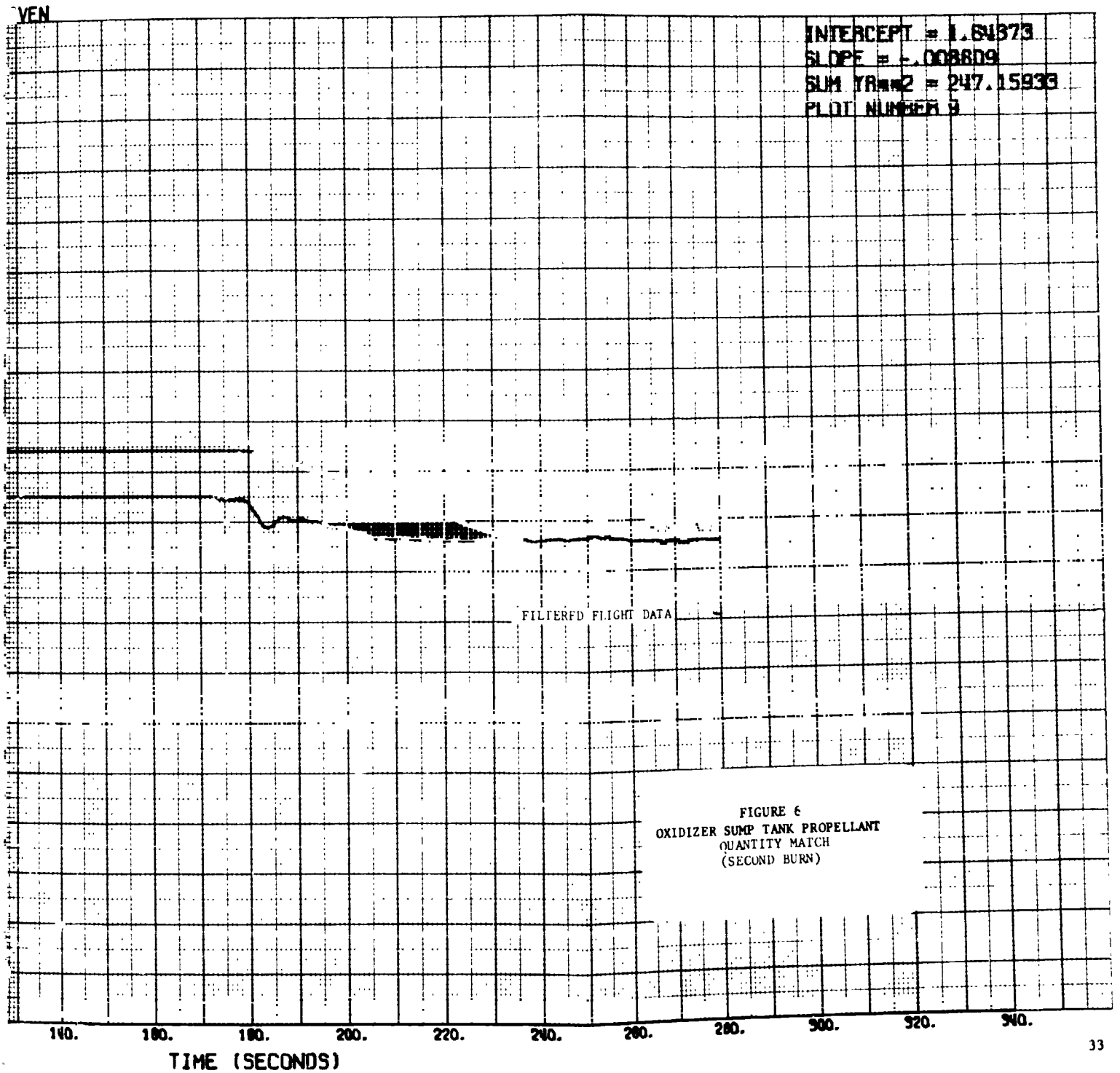

FIGURE 6
OXIDIZER SUMP TANK PROPELLANT
QUANTITY MATCH
(SECOND BURN)

FOLDOUT FRAME

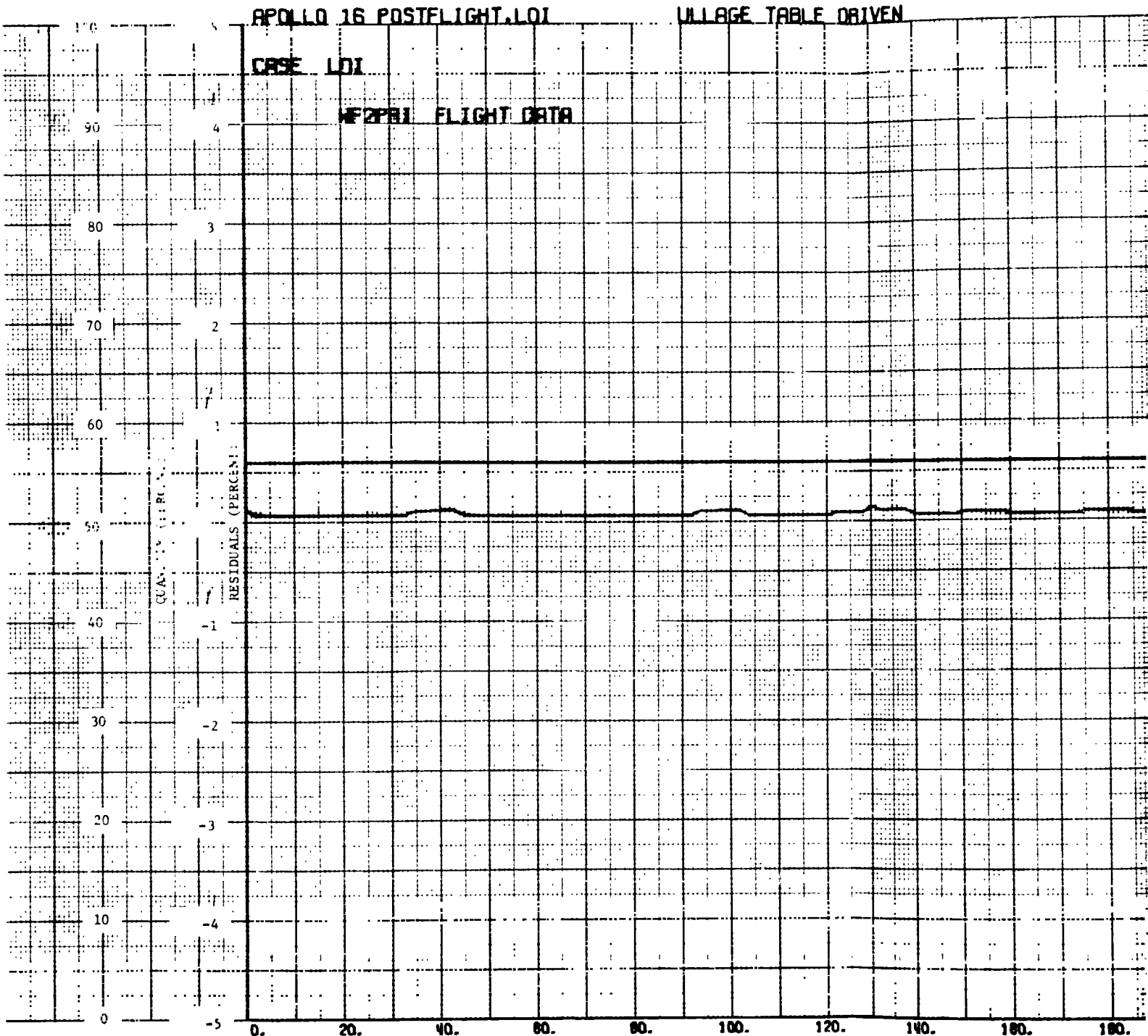

FOLDOUT FRAME 2

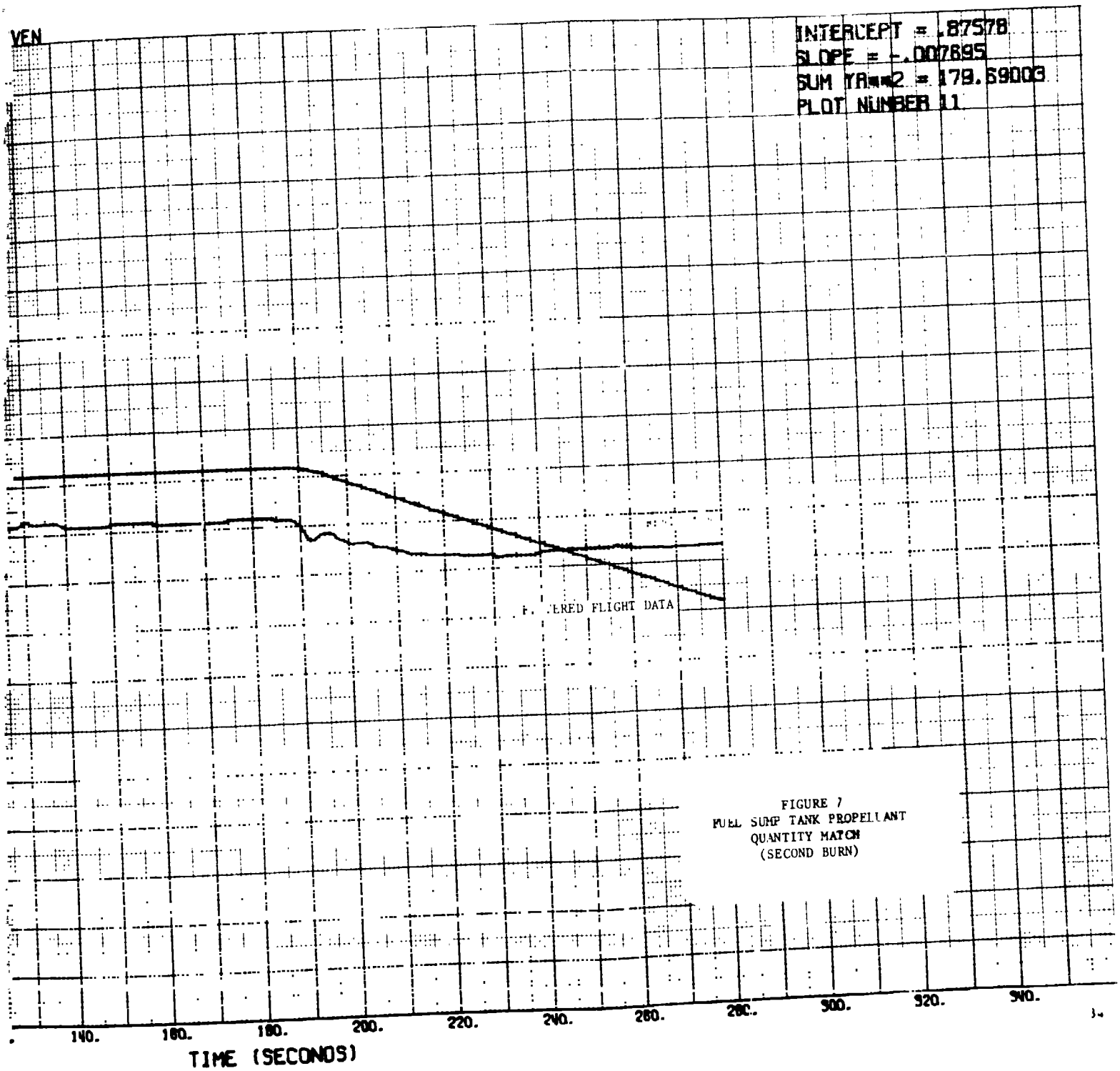

FIGURE 7
FUEL SUMP TANK PROPELLANT
QUANTITY MATCH
(SECOND BURN)

)LDOUT FRAME

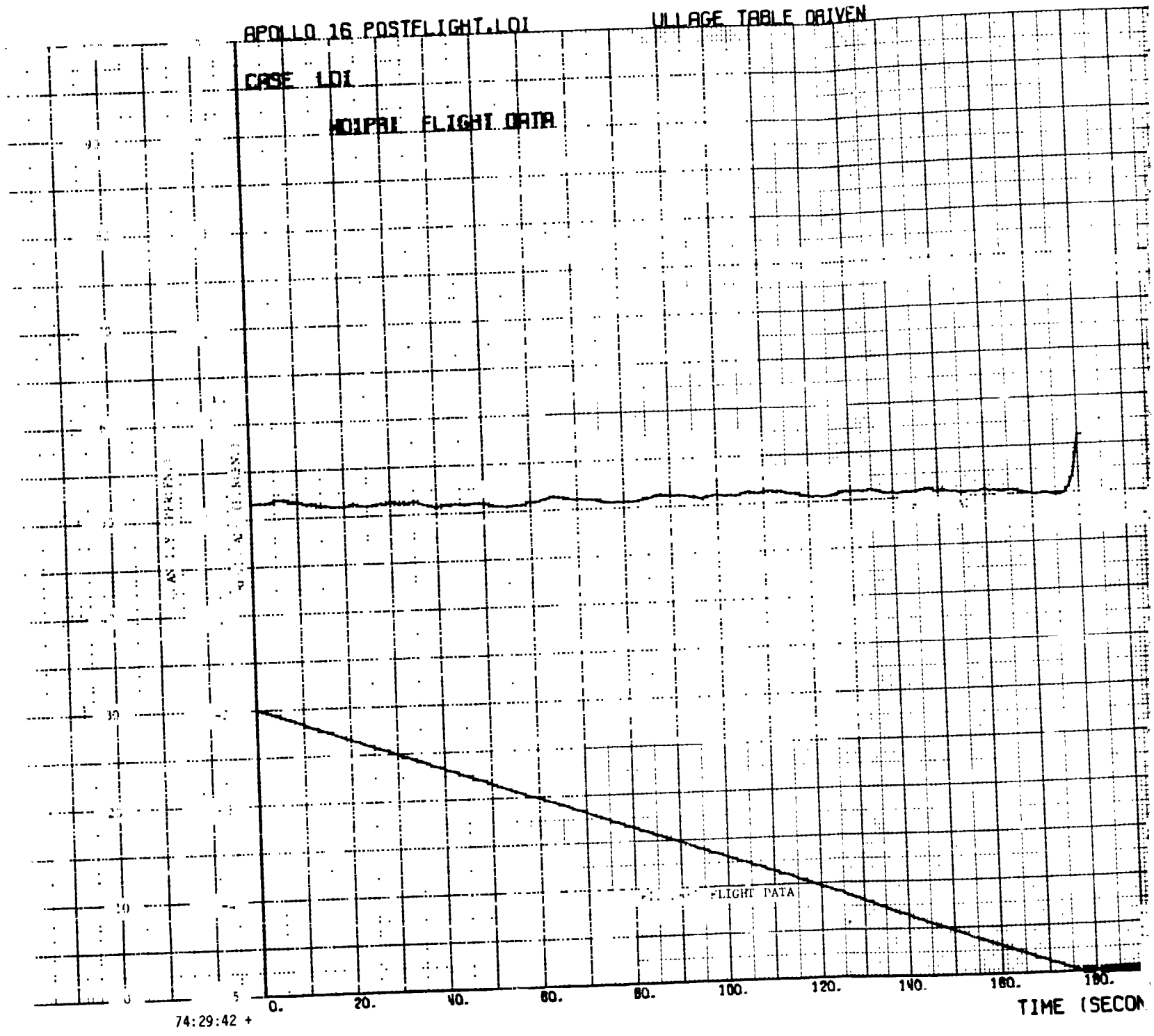
APOLLO 16 POSTFLIGHT.LOI
ULLAGE TABLE DRIVEN
CASE LOI
NOMPAR FLIGHT DATA
FLIGHT DATA
0.
20.
40.
60.
80.
100.
120.
140.
160.
180.
TIME (SECON
74:29:42 +

FOLDOUT FRAME 2

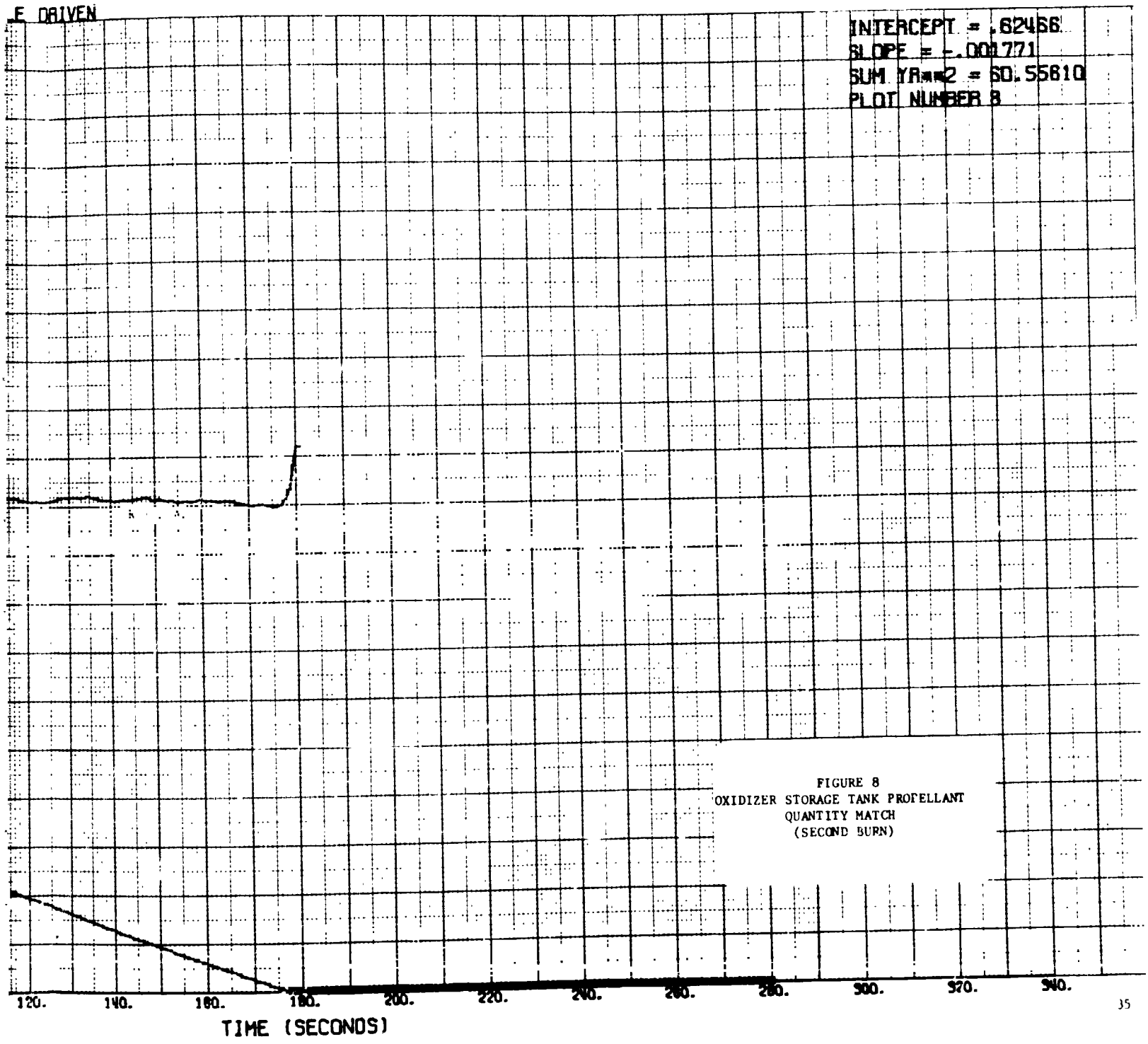

FIGURE 8
OXIDIZER STORAGE TANK PROPELLANT
QUANTITY MATCH
(SECOND BURN)

FOLDOUT FRAME

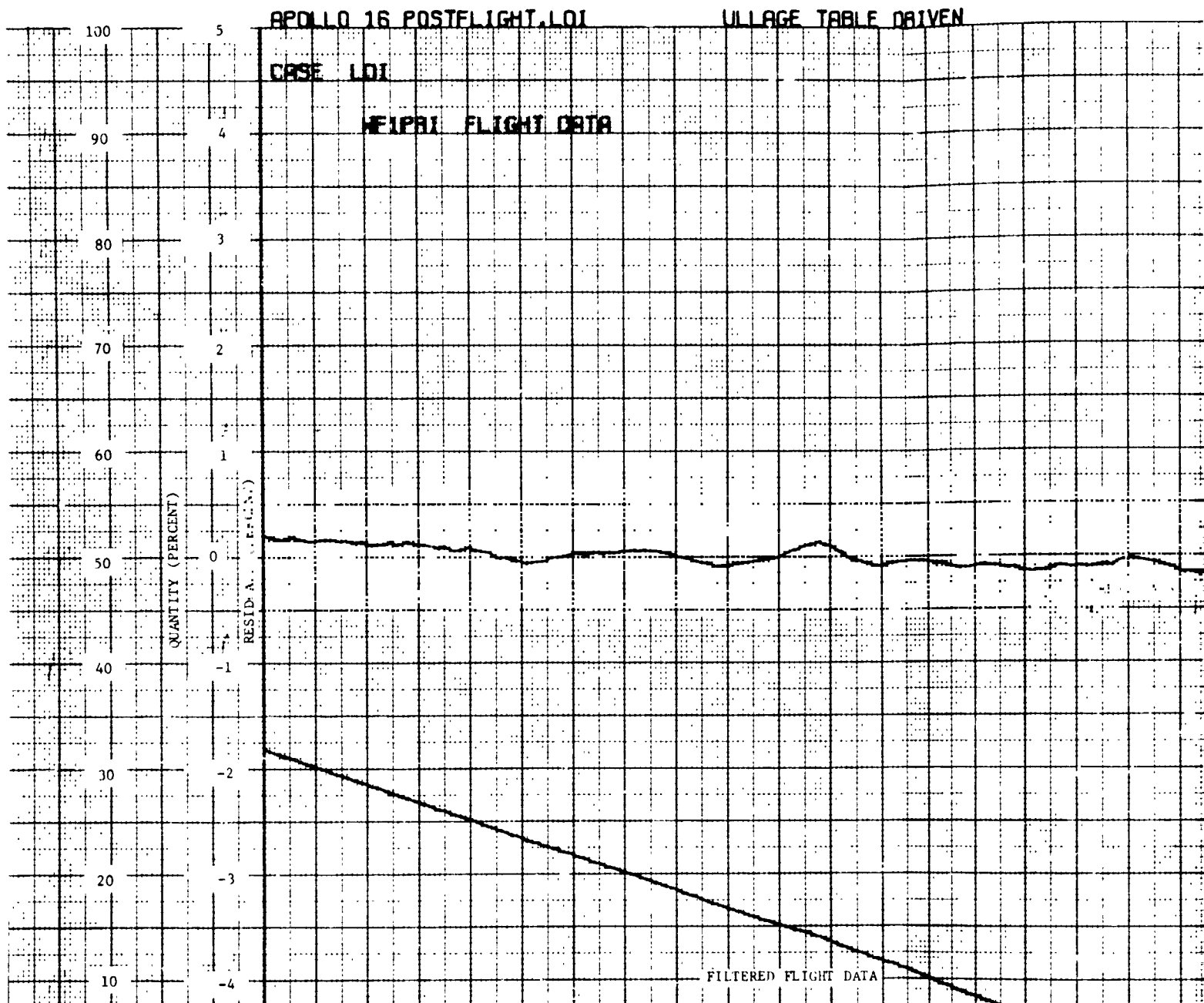

FOLDOUT FRAME 2

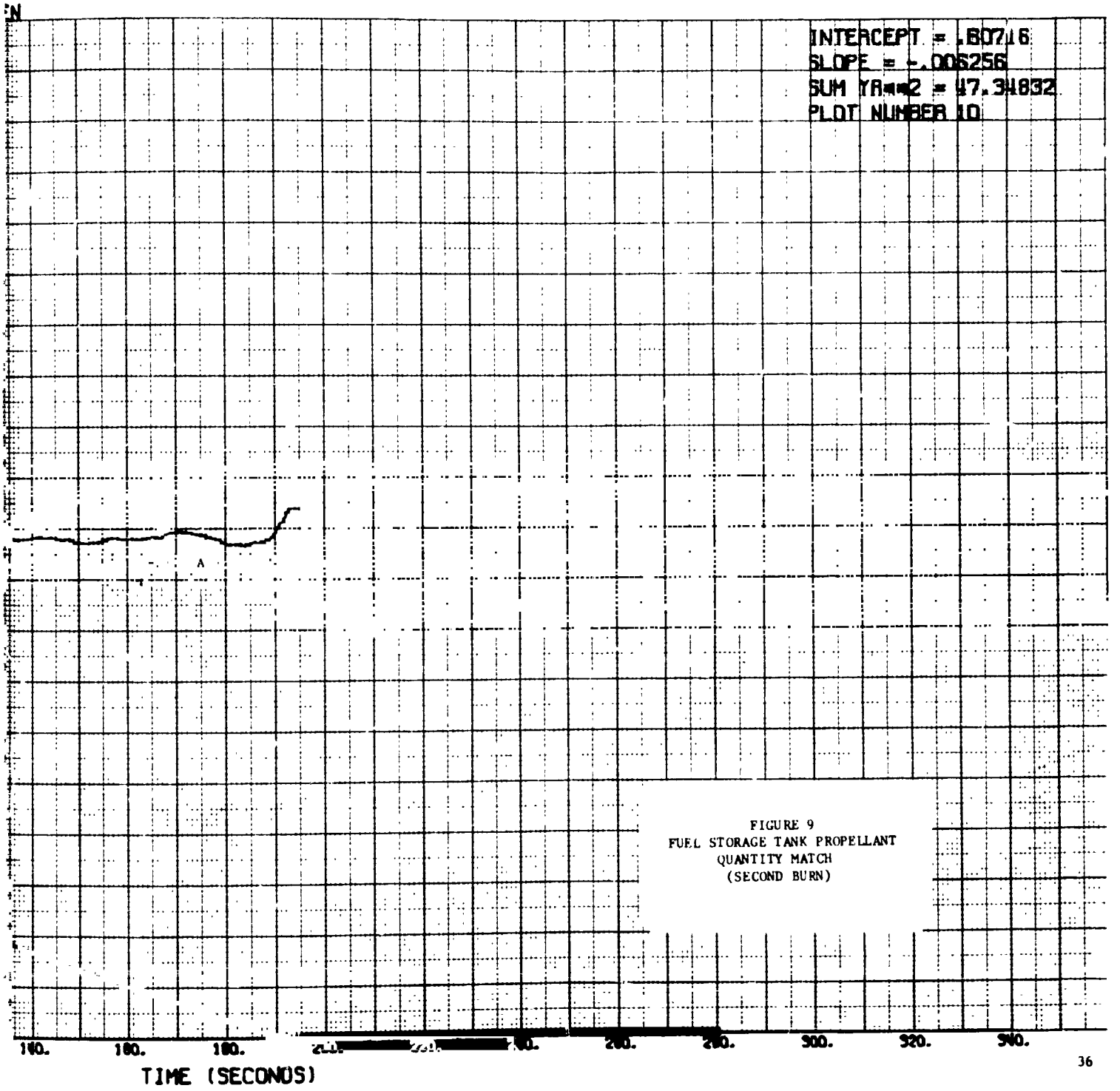

FIGURE 9
FUEL STORAGE TANK PROPELLANT
QUANTITY MATCH
(SECOND BURN)

FOLDOUT FRAME 1

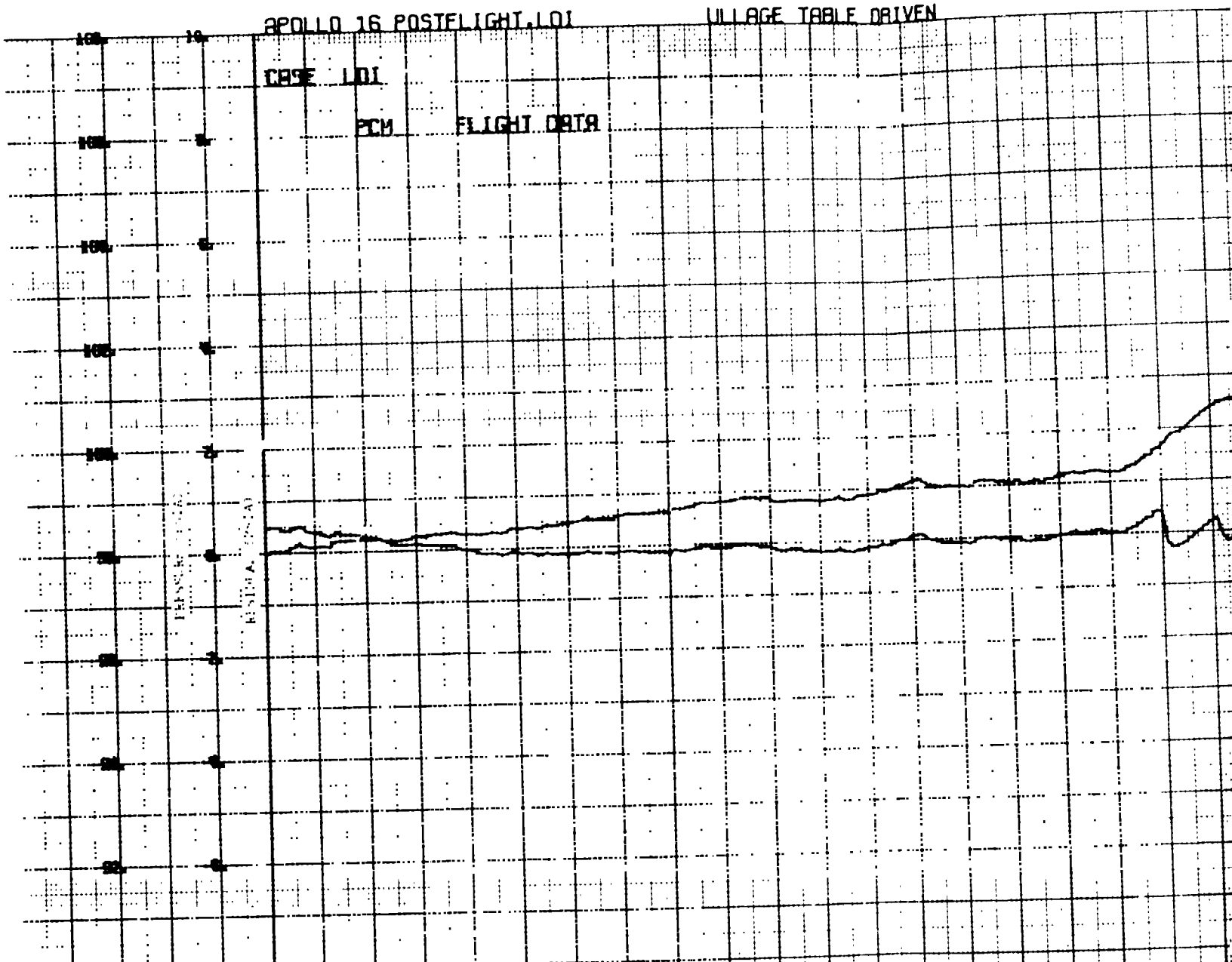

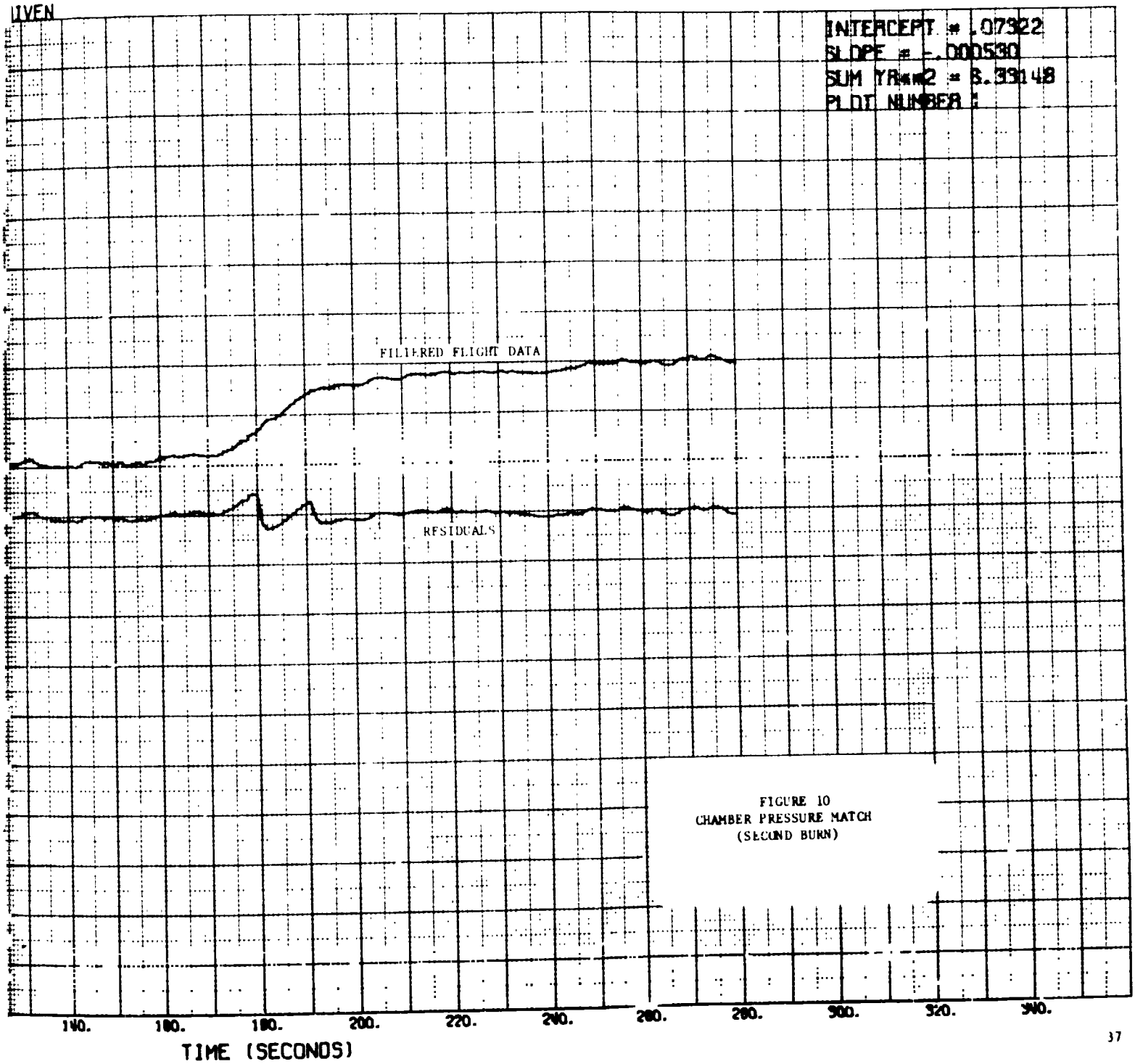

FIGURE 10
CHAMBER PRESSURE MATCH
(SECOND BURN)

FOLDOUT FRAME

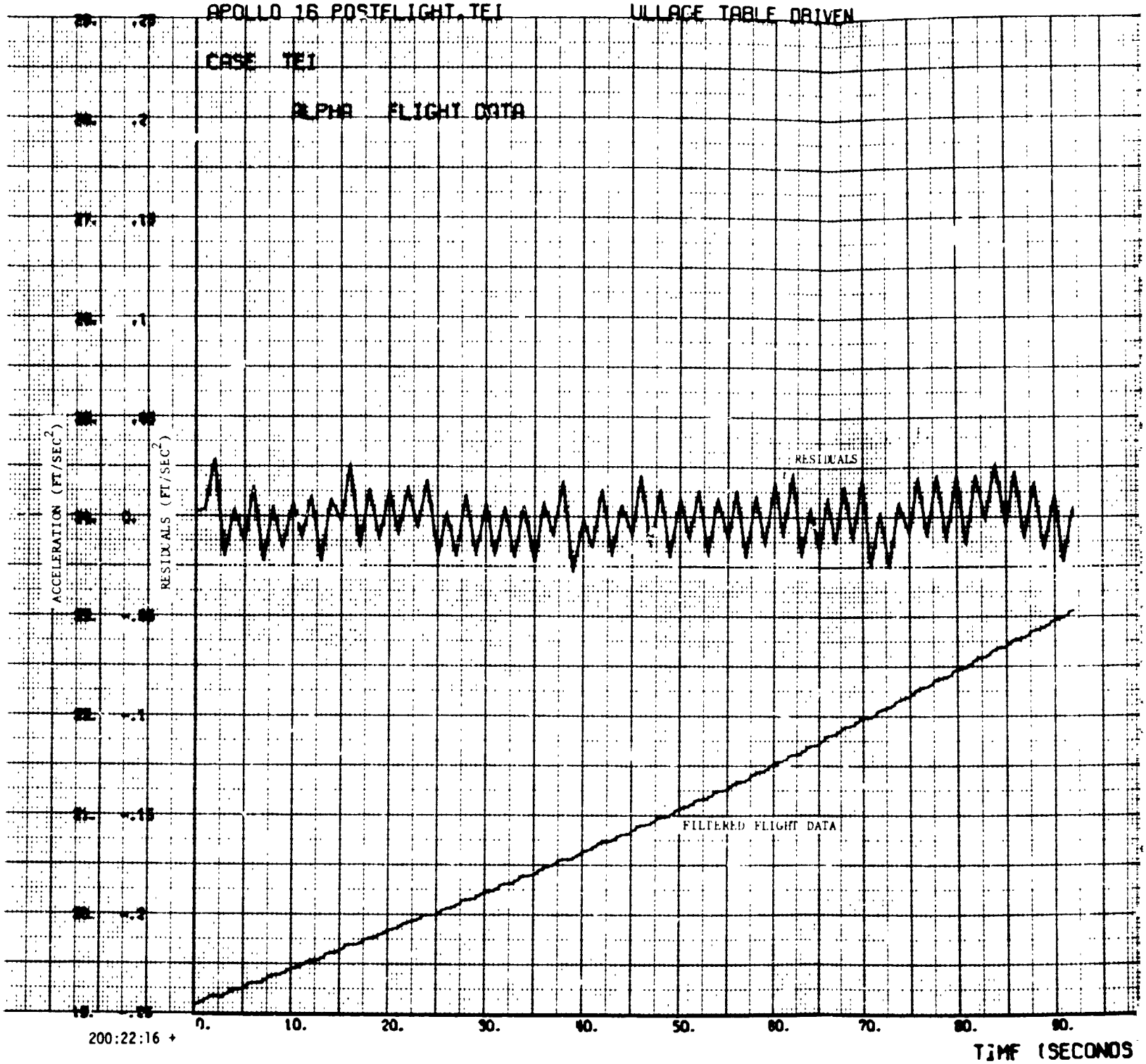

FOLDOUT FRAME 2

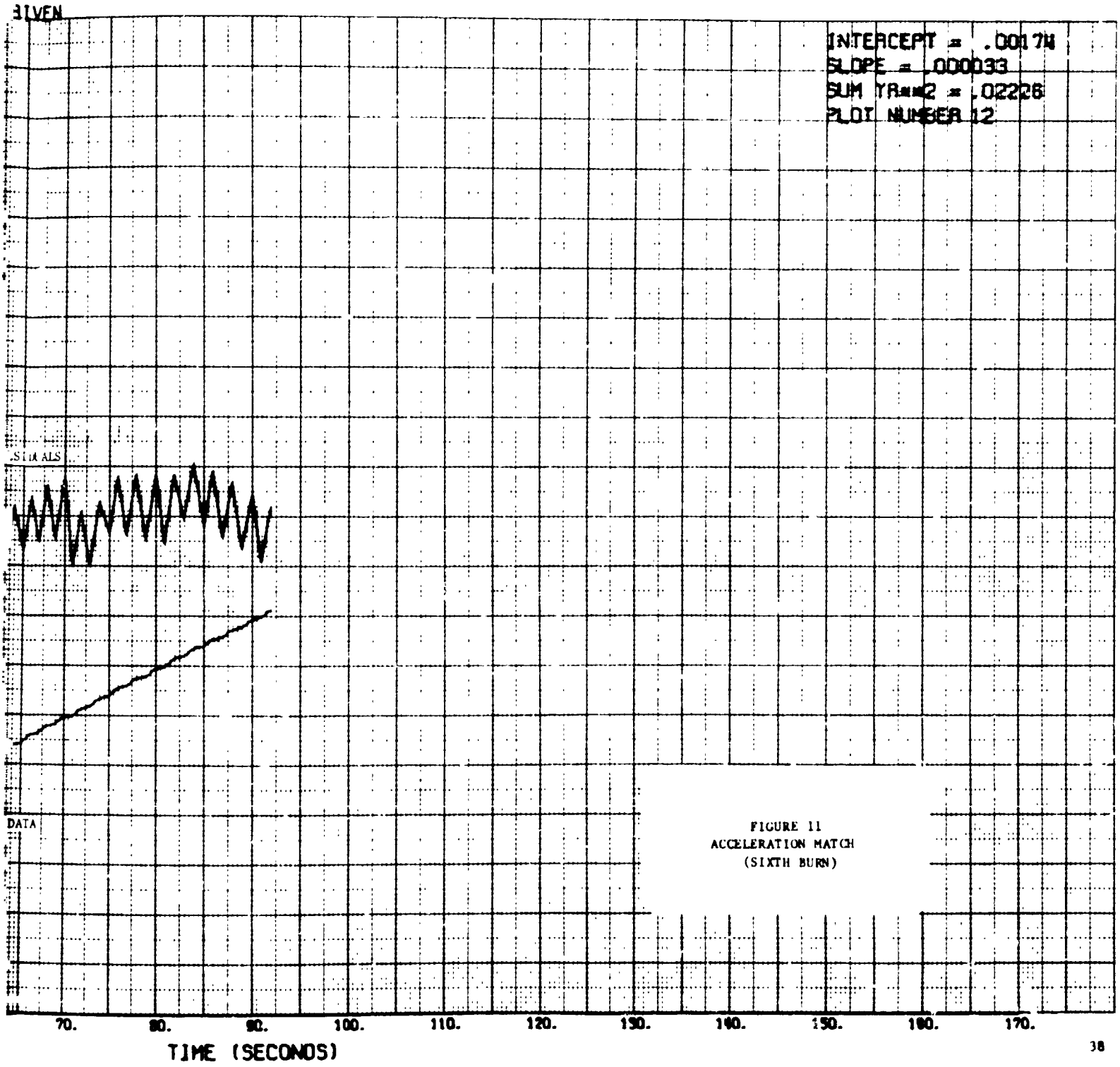

FIGURE 11
ACCELERATION MATCH
(SIXTH BURN)

FOLDOUT FRAME

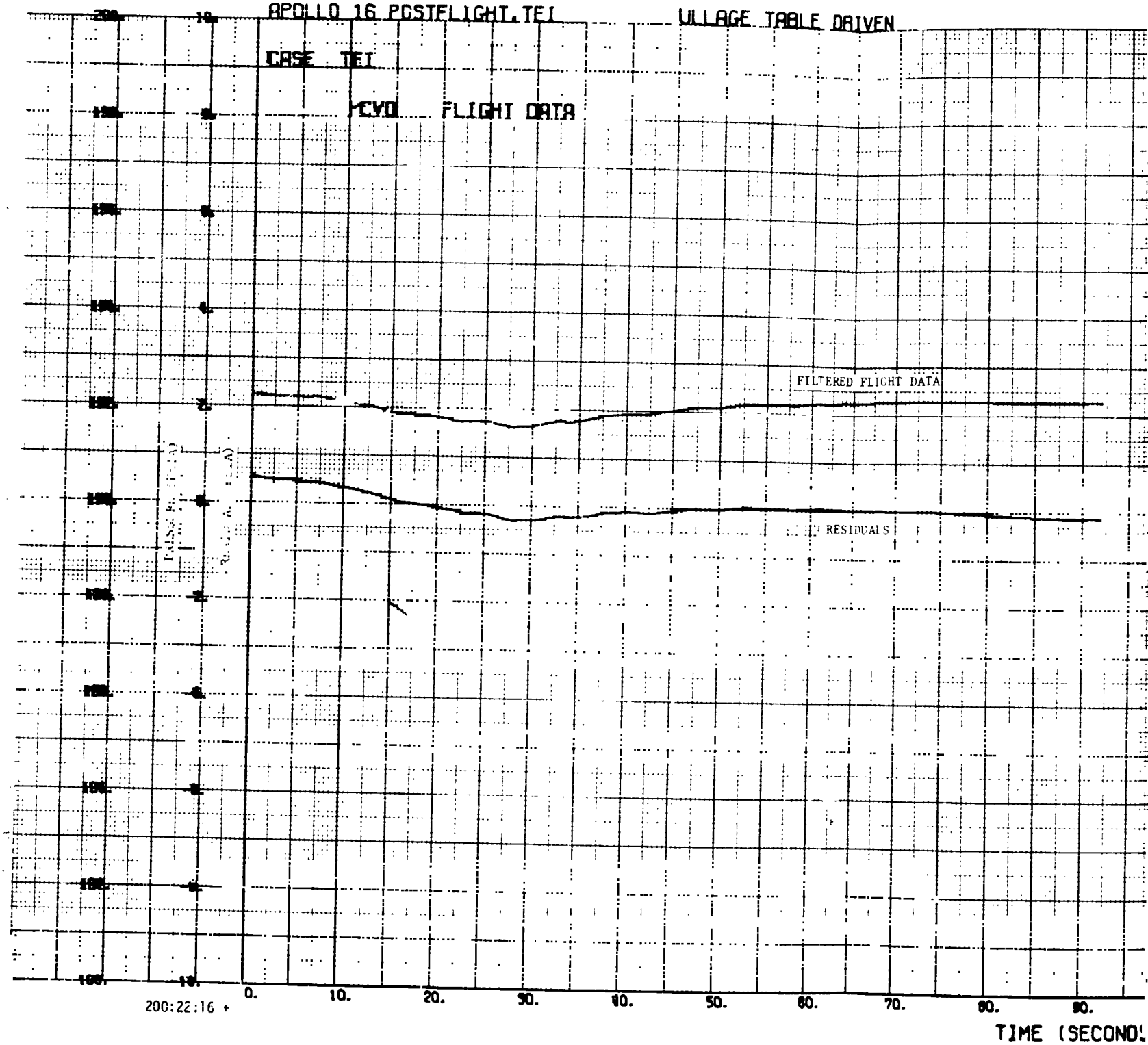

FOLDOUT FRAME 2

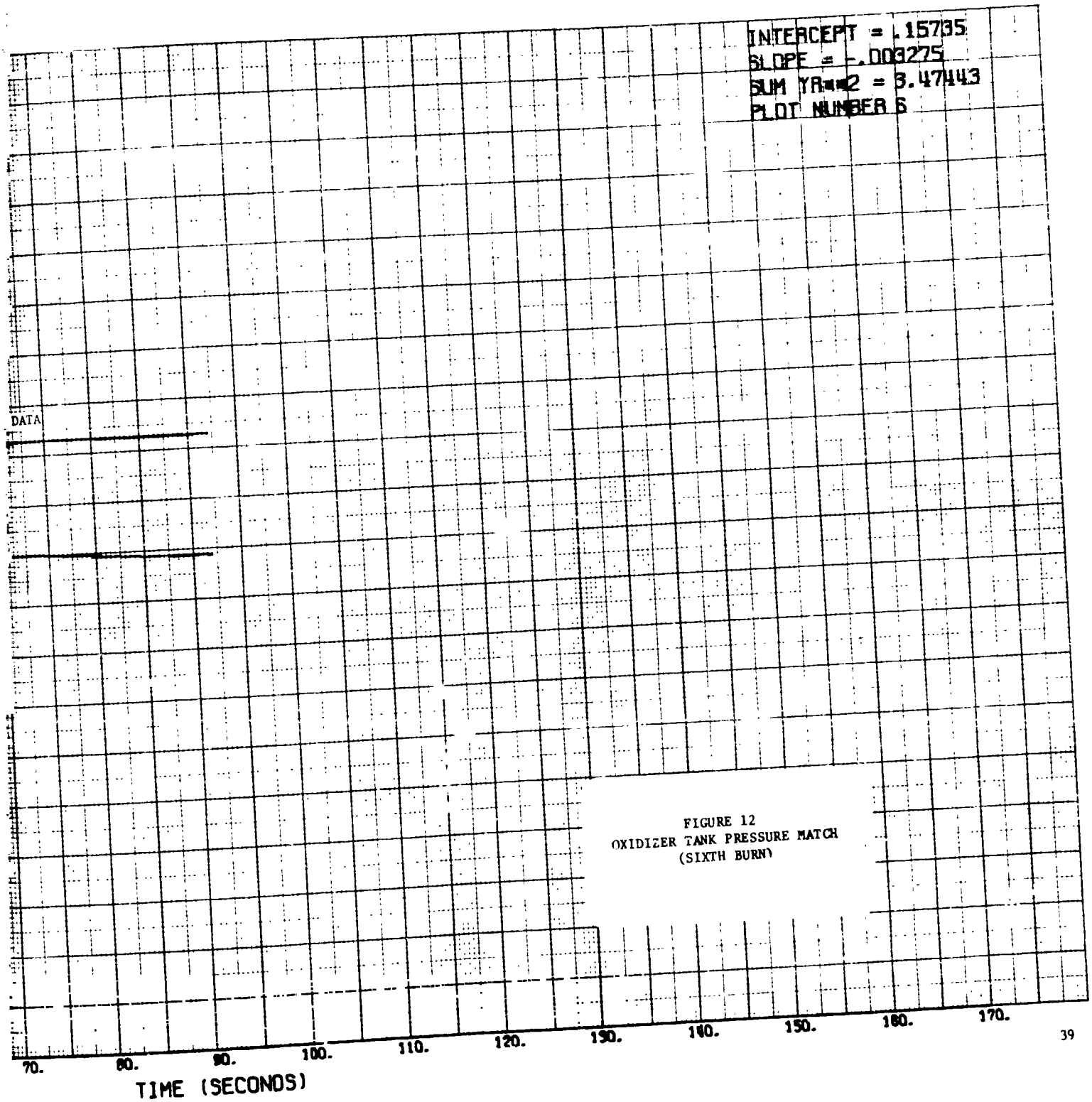

FIGURE 12
OXIDIZER TANK PRESSURE MATCH
(SIXTH BURN)

FOLDOUT FRAME

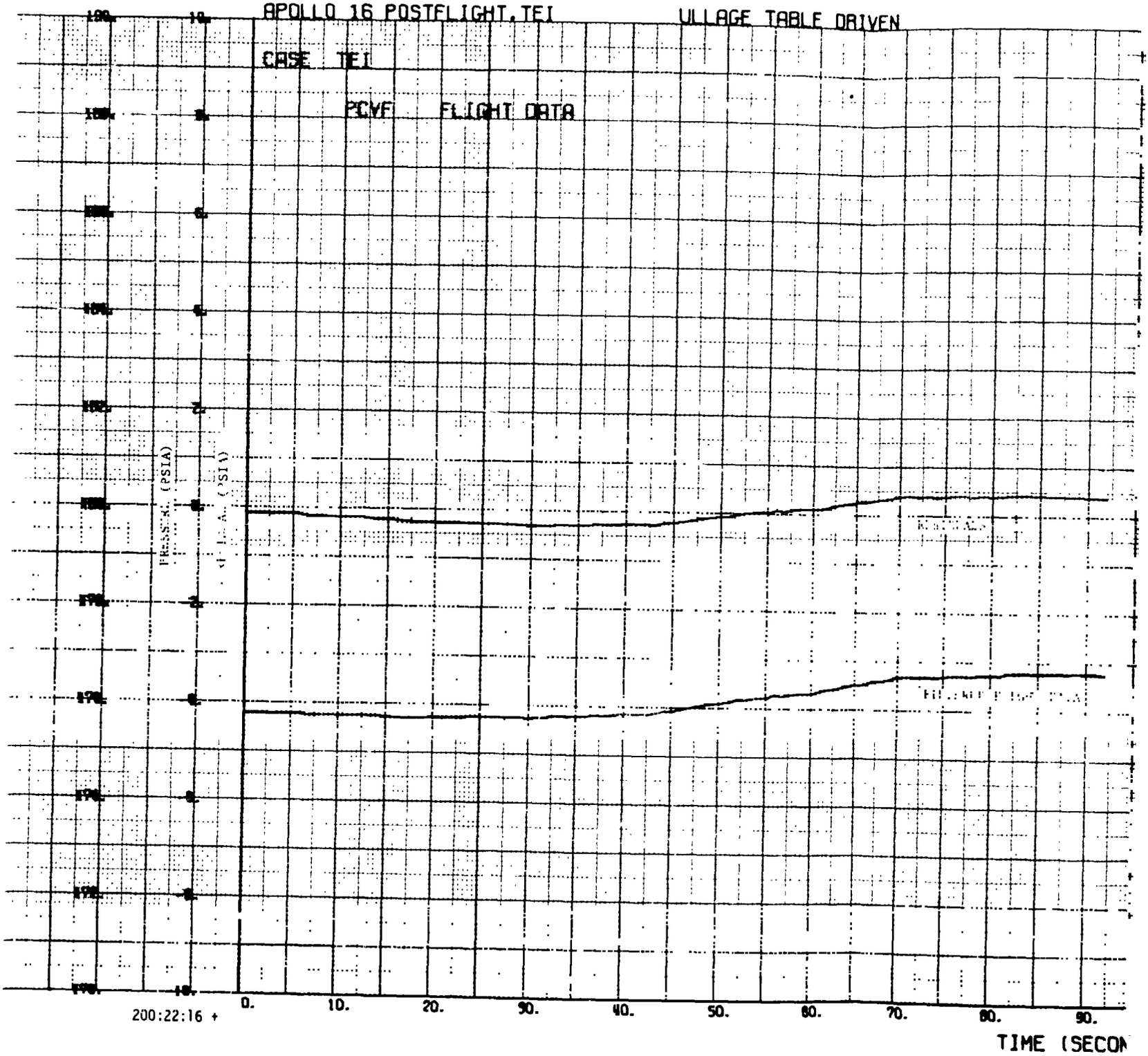

FOLDOUT FRAME 2

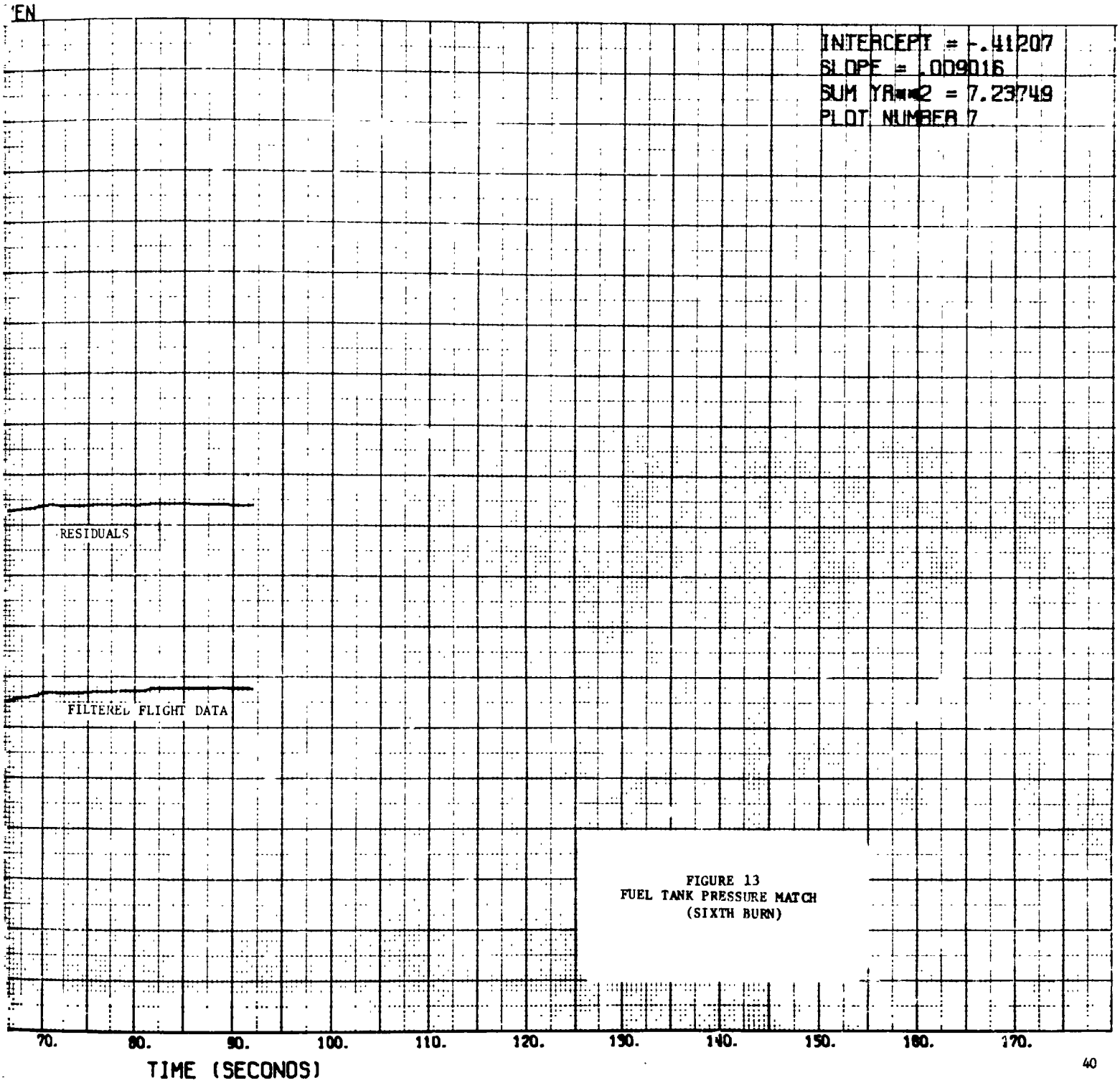

FIGURE 13
FUEL TANK PRESSURE MATCH
(SIXTH BURN)

FOLDOUT FRAME 1

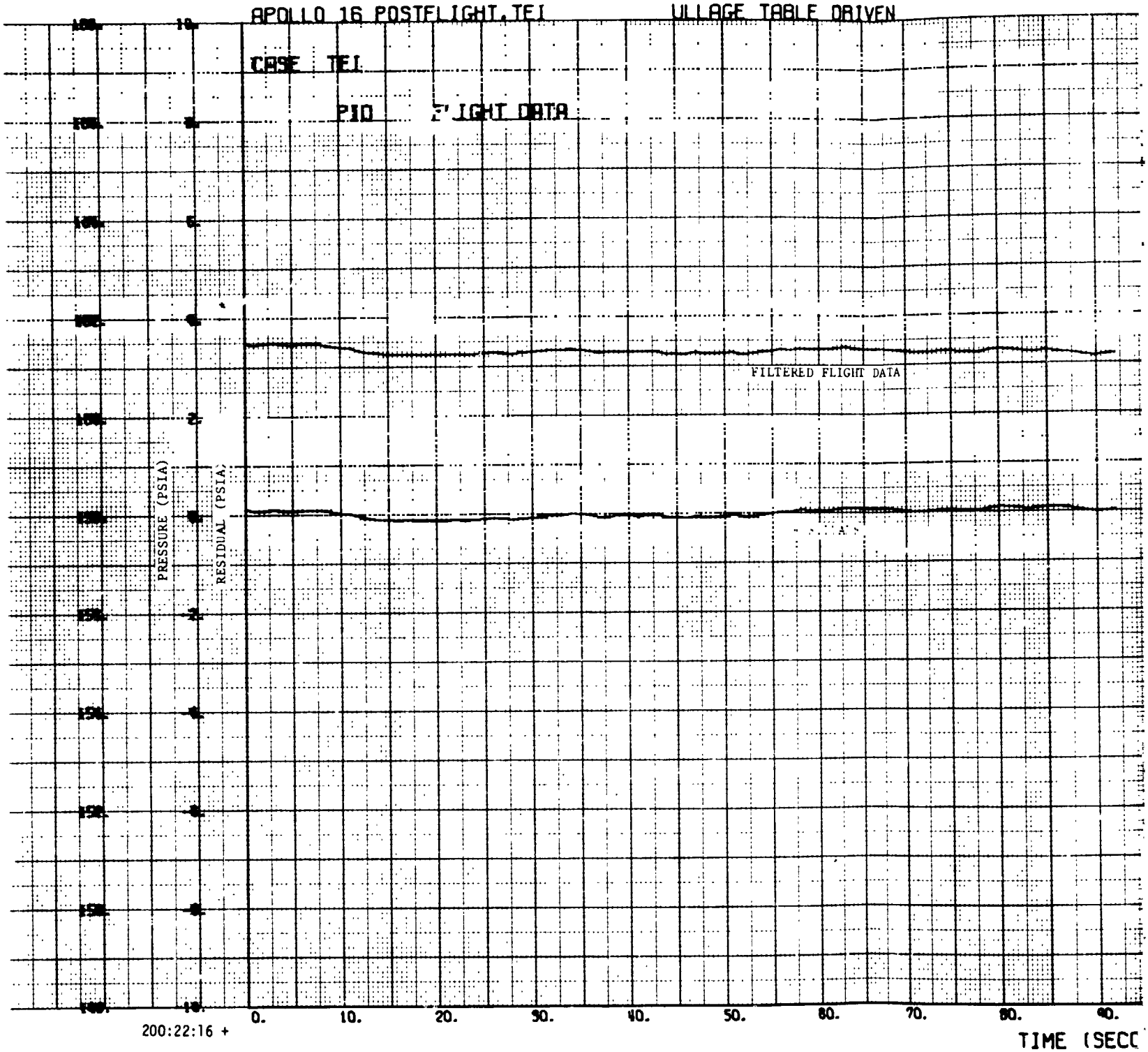

FOLDOUT FRAME 2

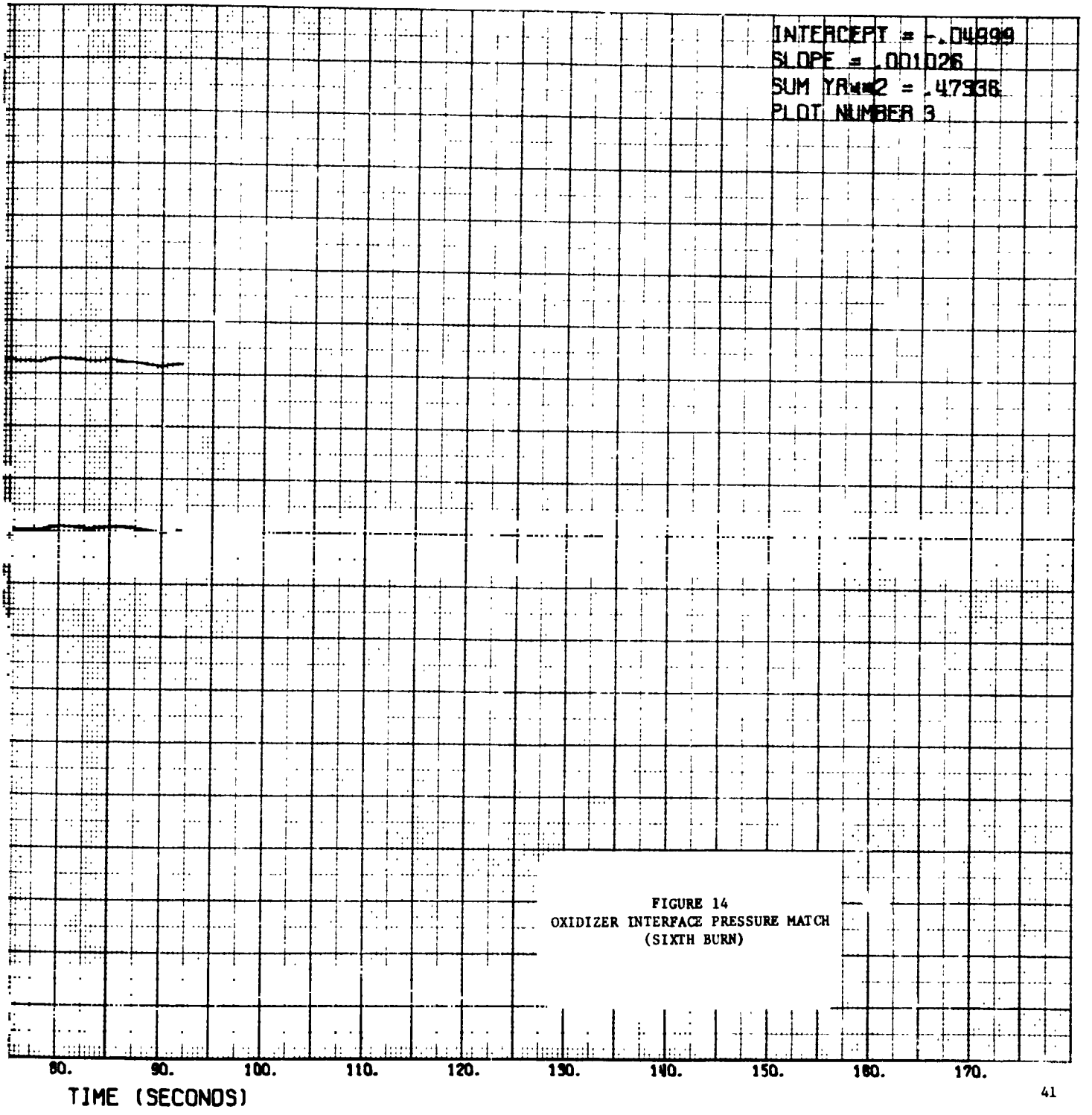

FIGURE 14
OXIDIZER INTERFACE PRESSURE MATCH
(SIXTH BURN)

FOLDOUT FRAME

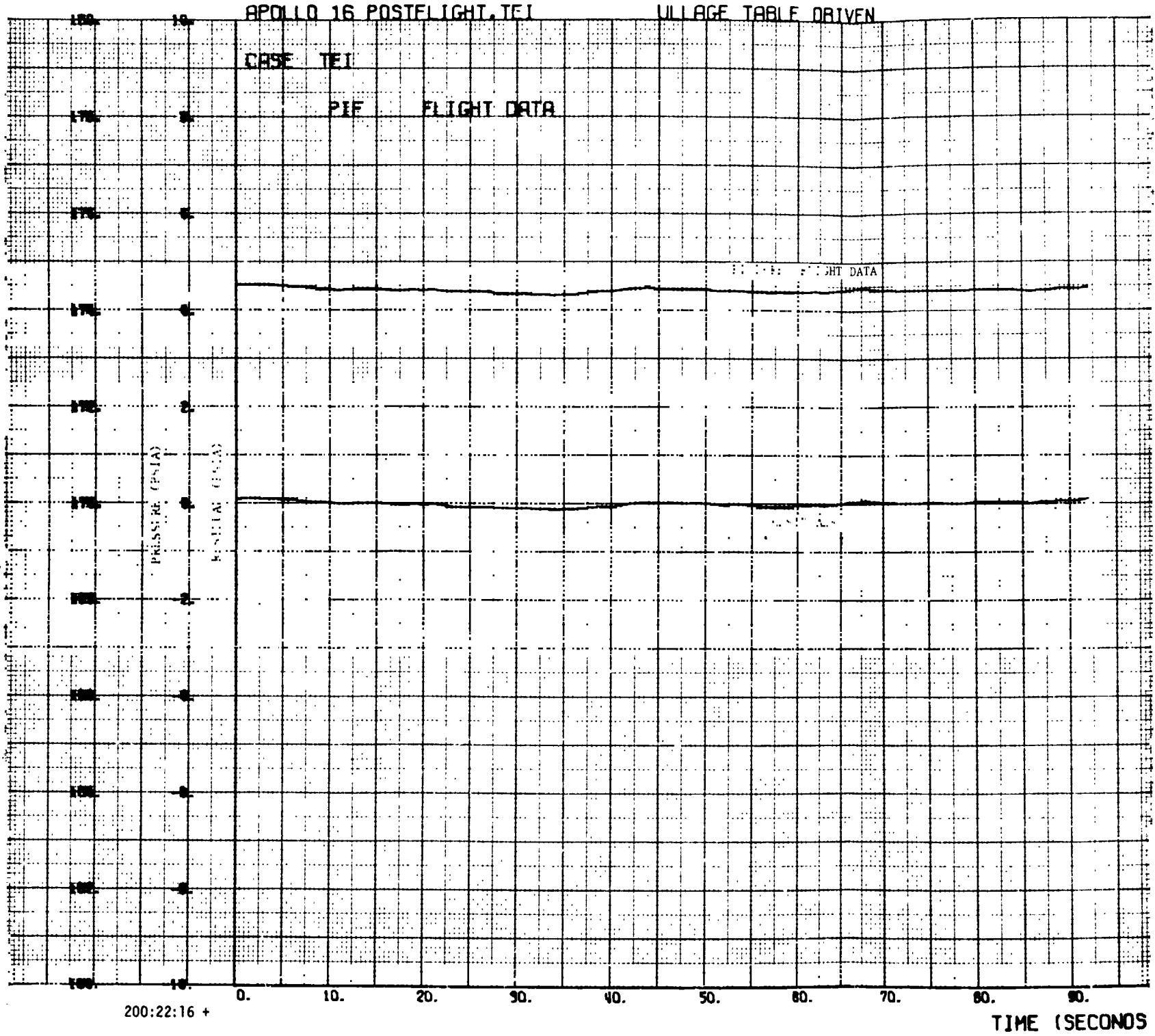

FOLDOUT FRAME 2

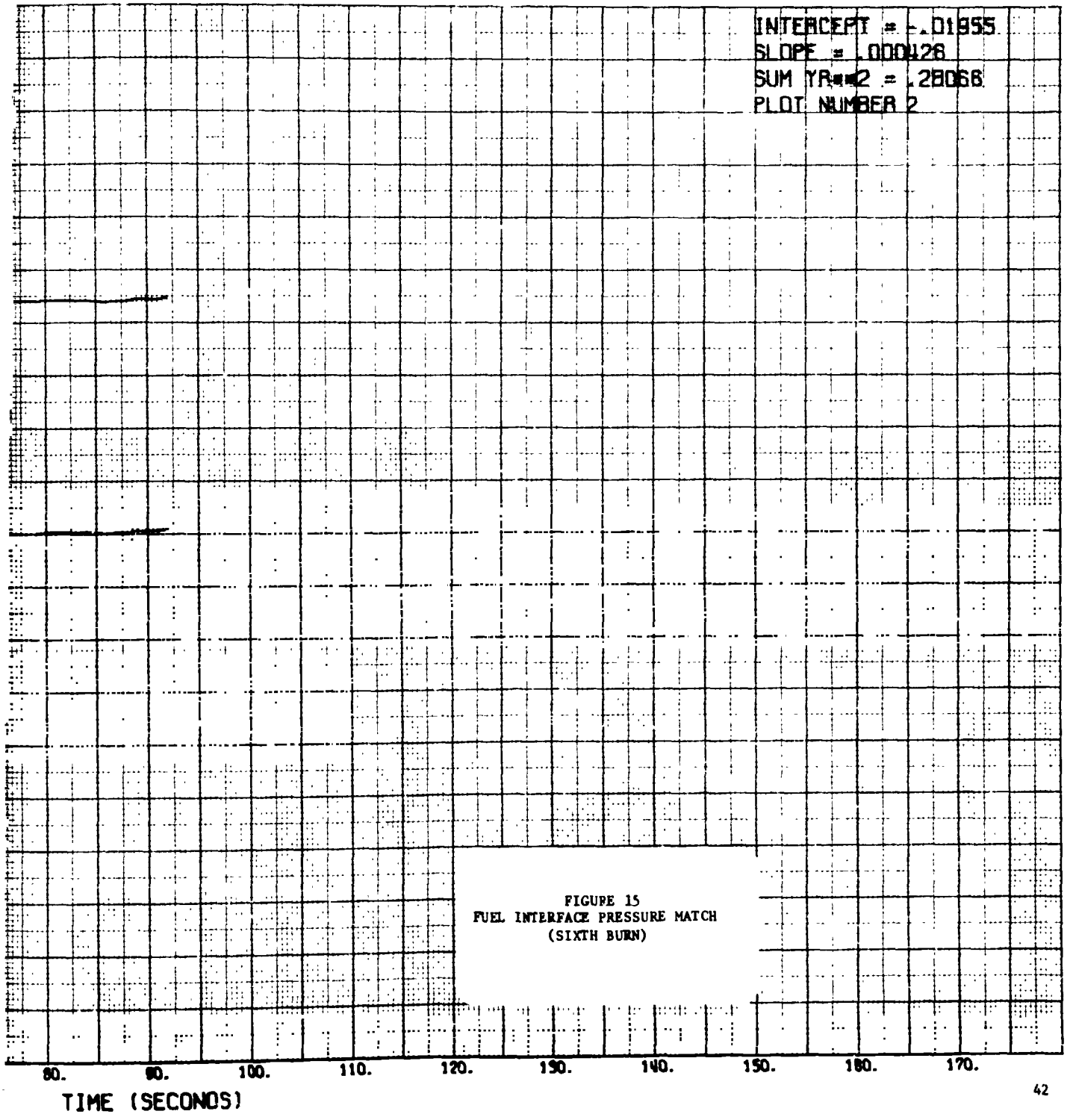

FIGURE 15
FUEL INTERFACE PRESSURE MATCH
(SIXTH BURN)

FOLDOUT FRAME

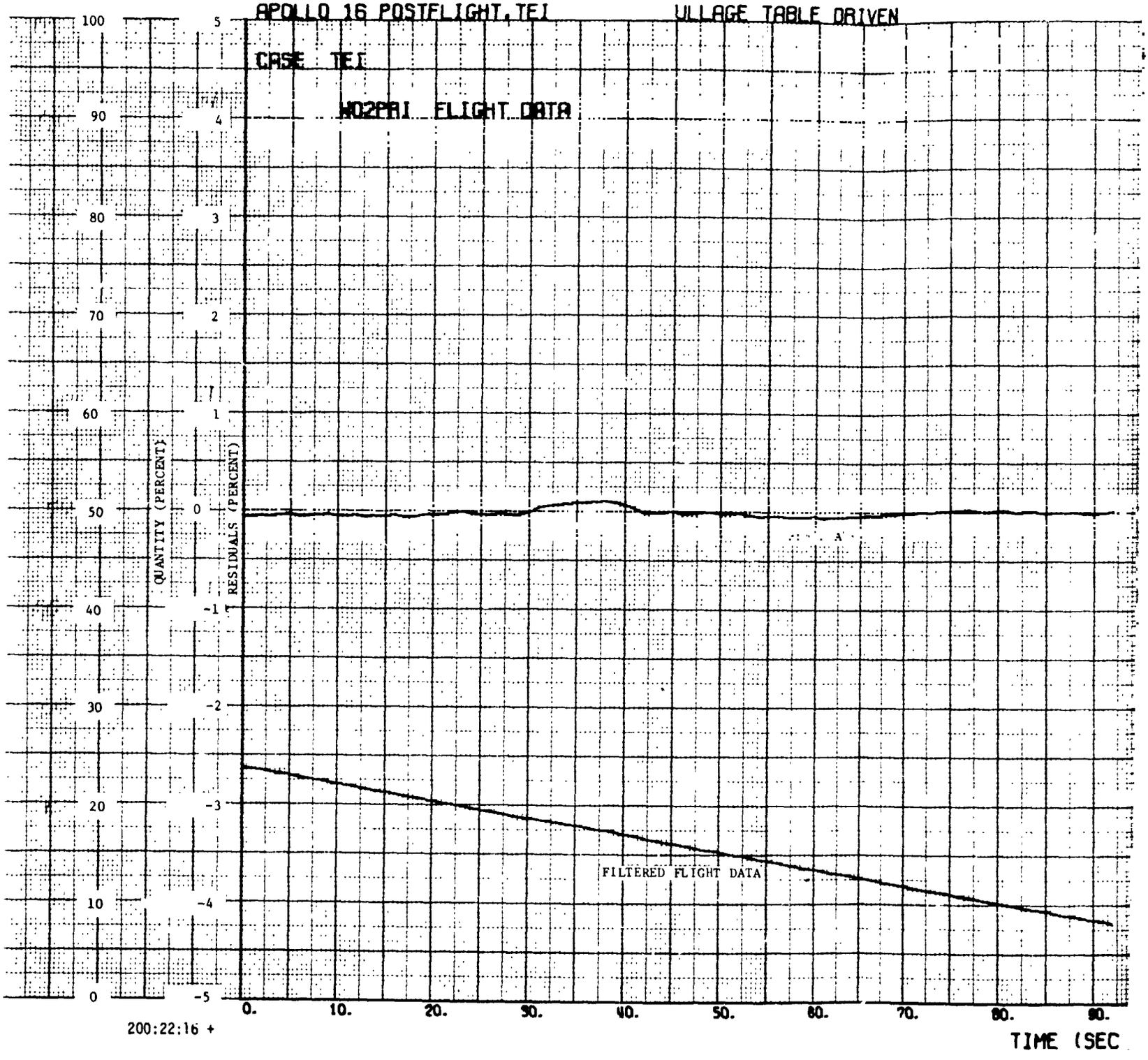

FOLDOUT FRAME 2

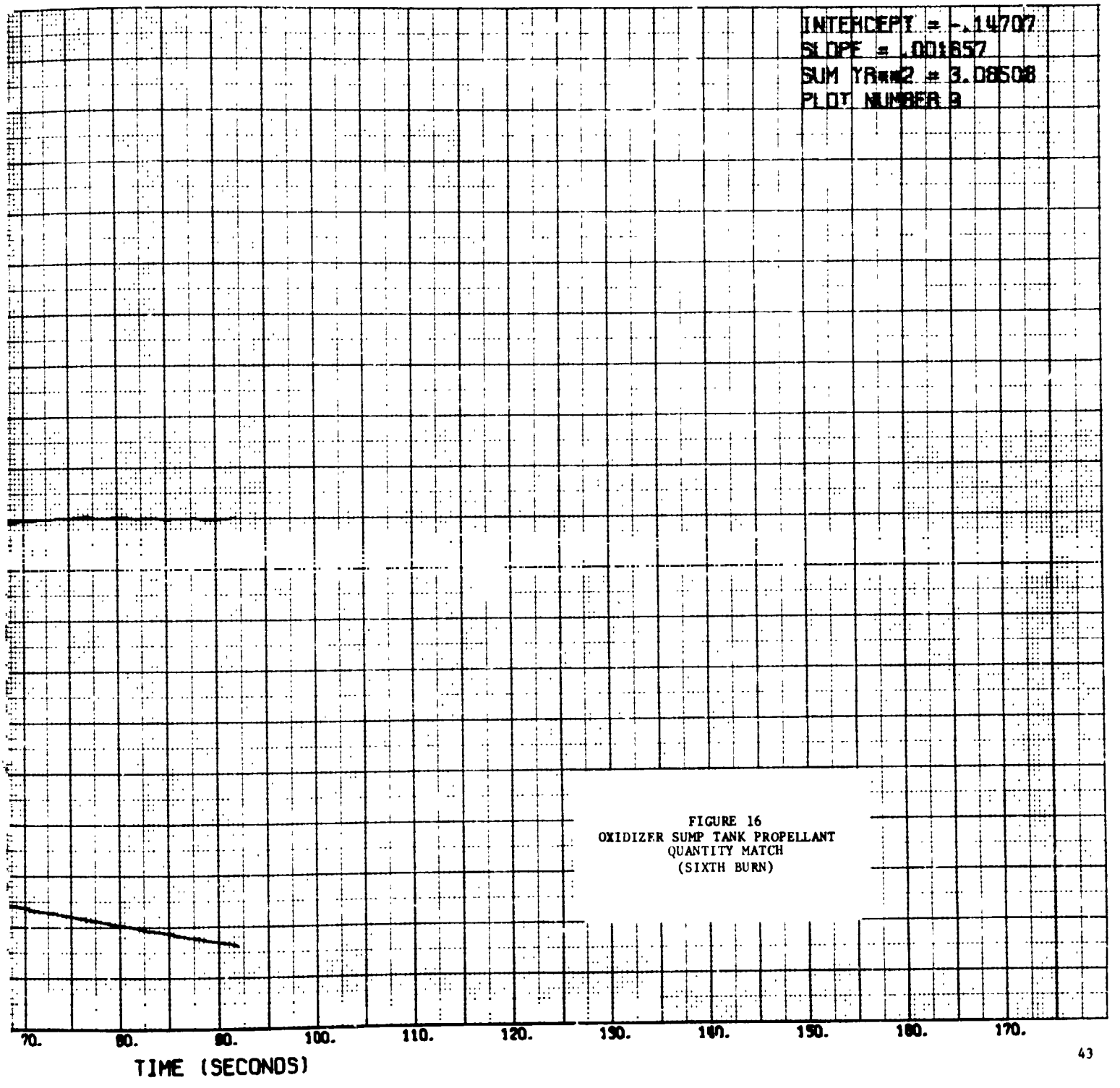

FIGURE 16
OXIDIZER SUMP TANK PROPELLANT
QUANTITY MATCH
(SIXTH BURN)

FOLDOUT FRAME

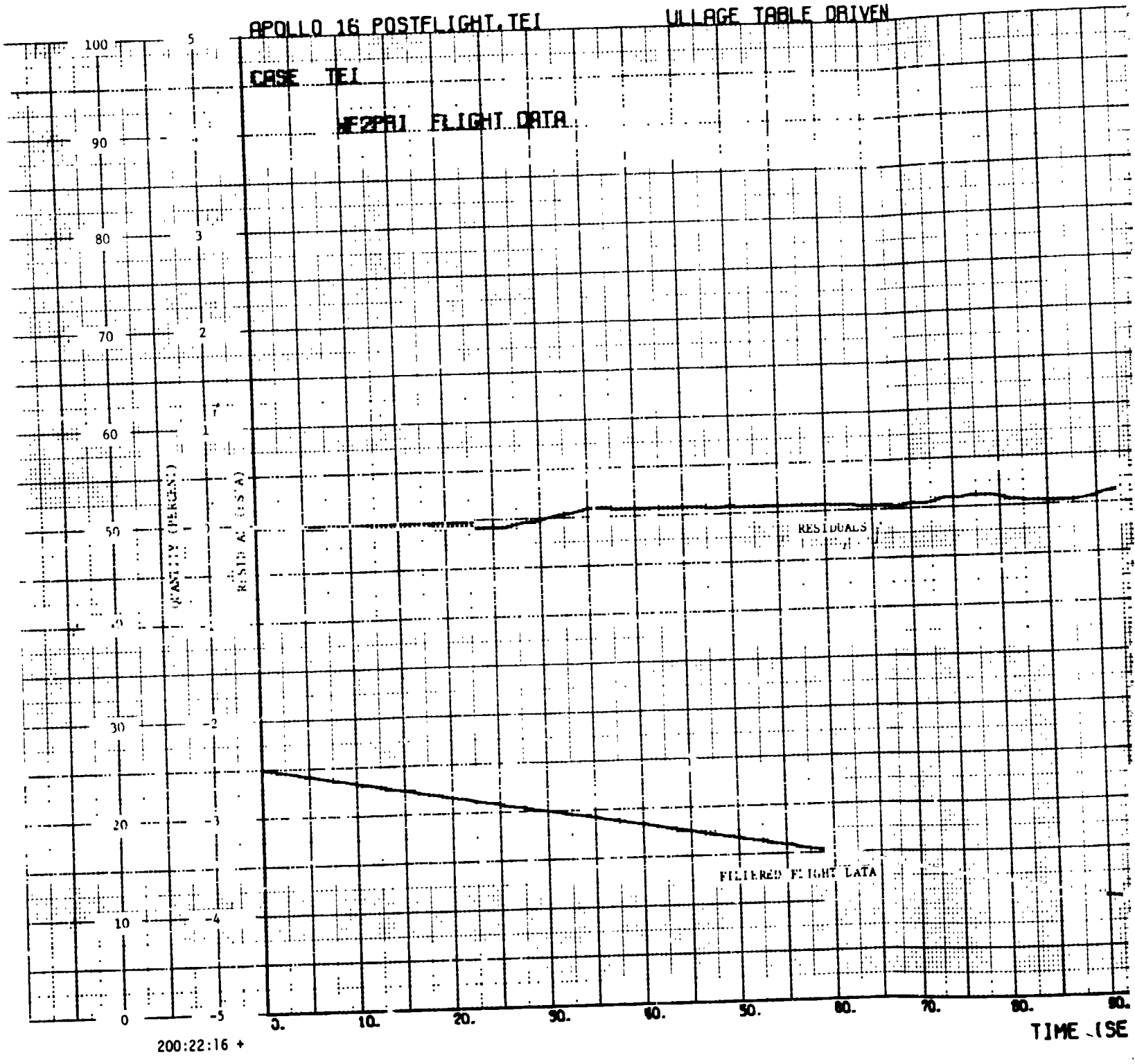

FOLDOUT FRAME 2

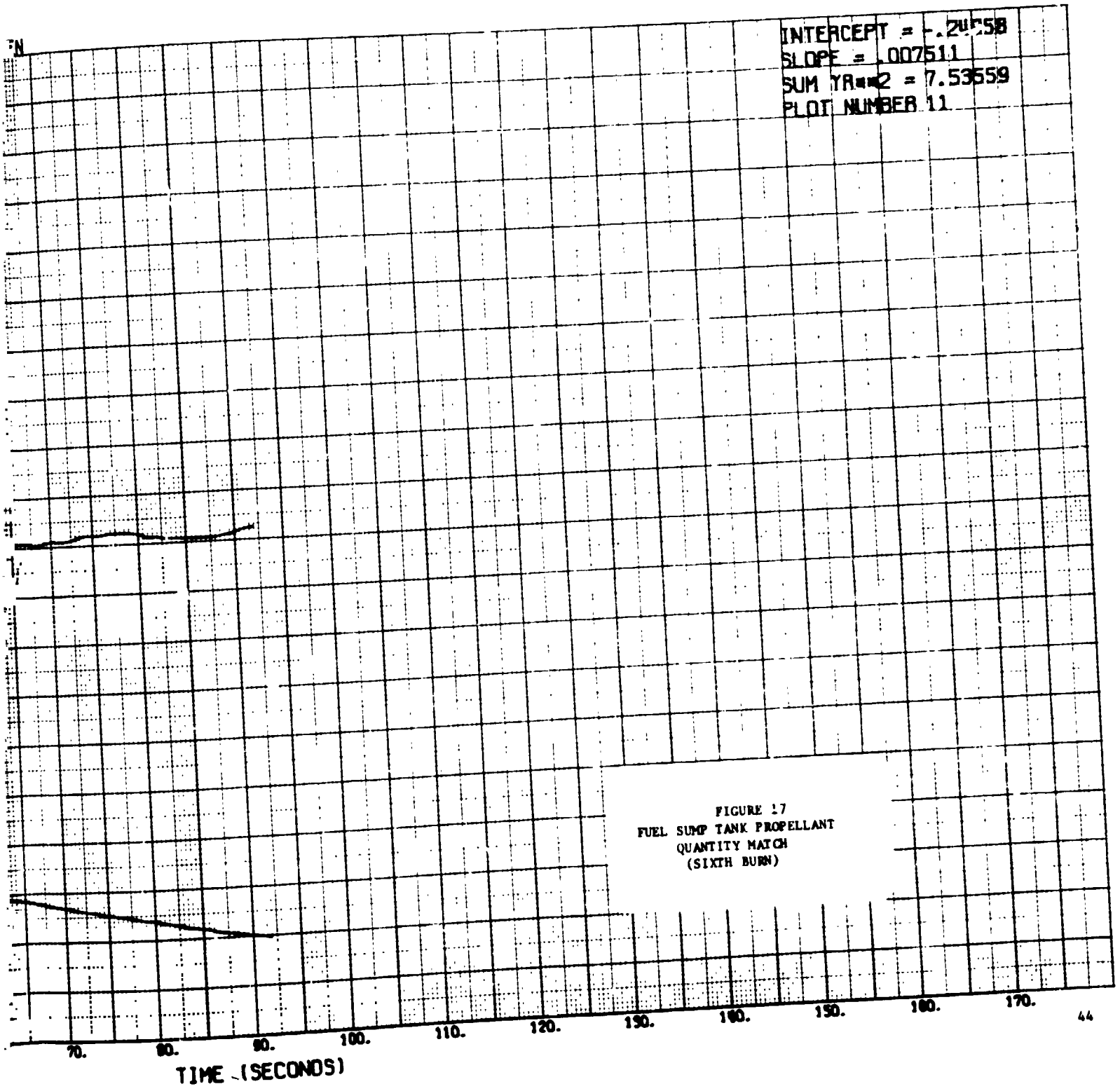

FIGURE 17
FUEL SUMP TANK PROPELLANT
QUANTITY MATCH
(SIXTH BURN)

FOLDOUT FRAME

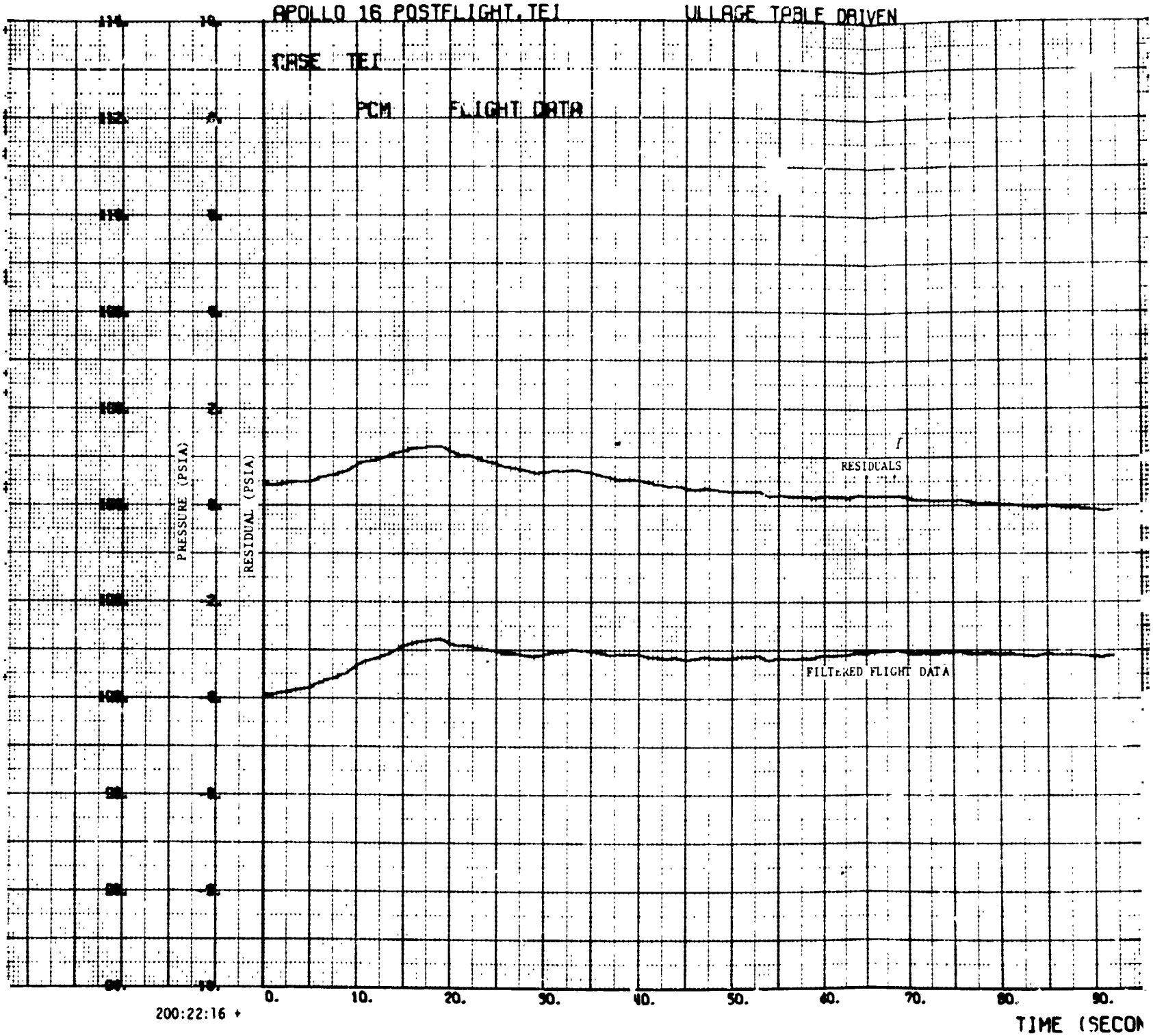

FOLDOUT FRAME 2

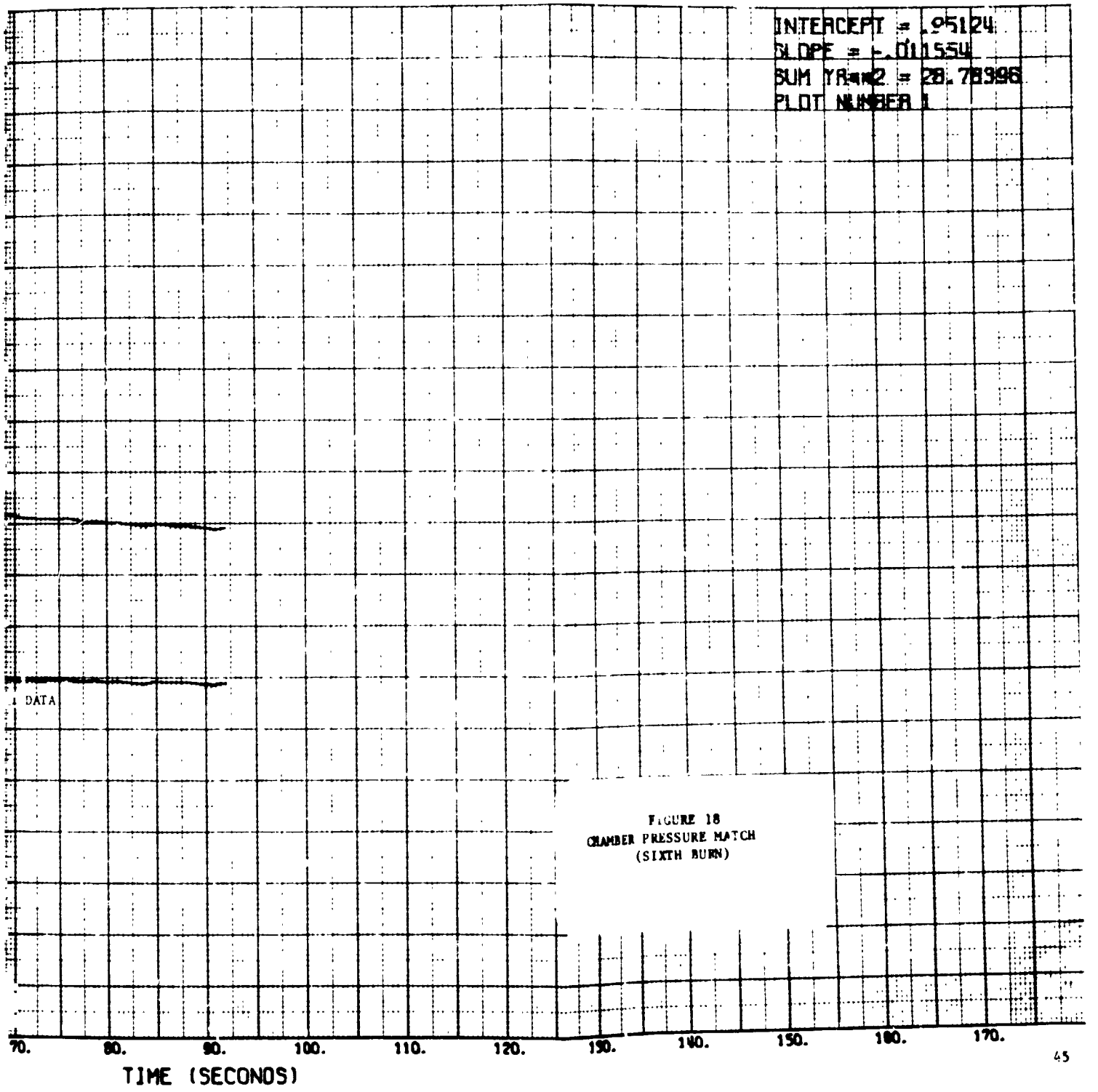

FIGURE 18
CHAMBER PRESSURE MATCH
(SIXTH BURN)

FOLDOUT FRAME

FIGURE 19

OXIDIZER INDICATED PROPELLANT UNBALA

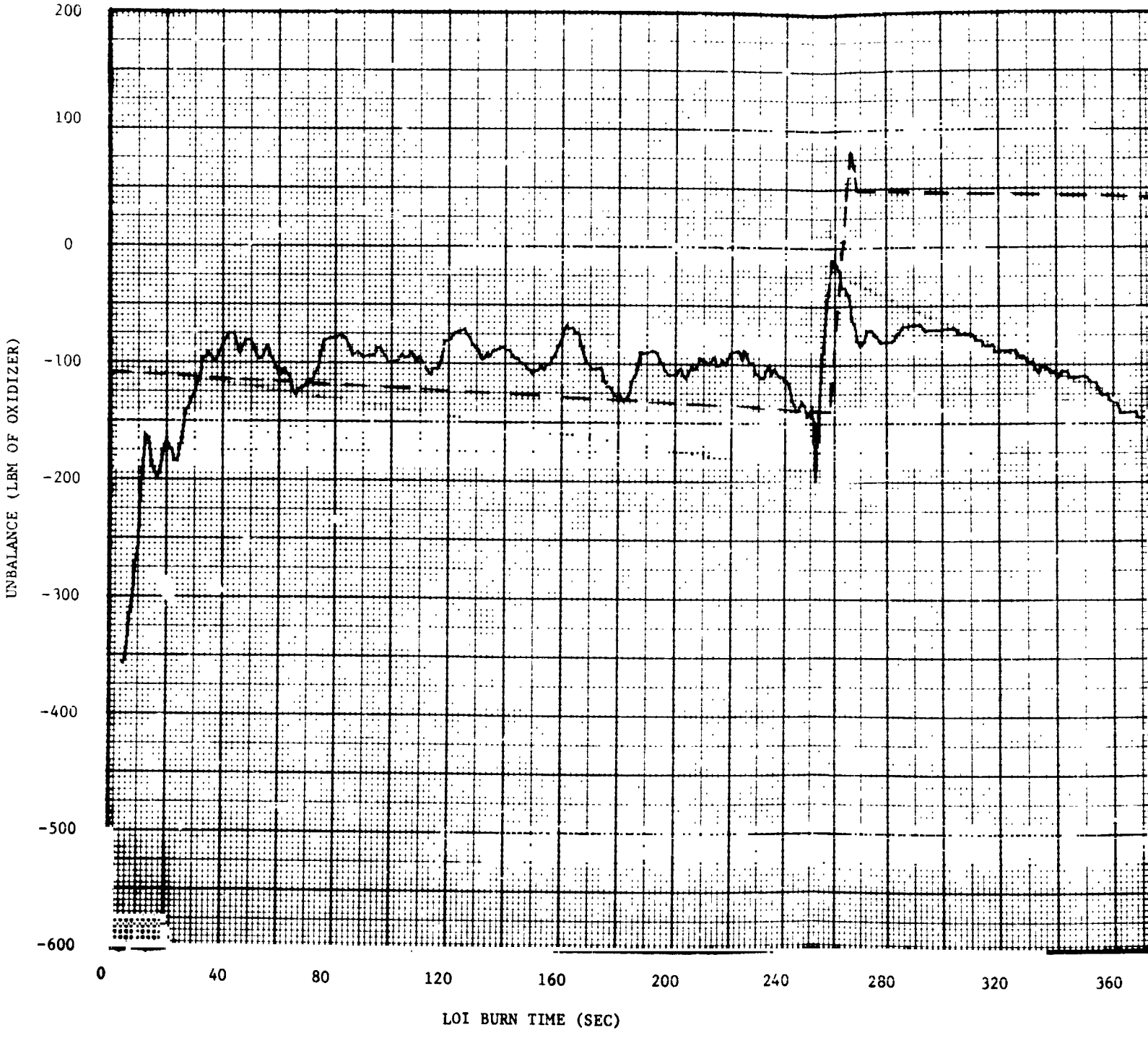

FIGURE 19

OXIDIZER INDICATED PROPELLANT UNBALANCE

FOLDOUT FRAME 2